JGR Biogeosciences

RESEARCH ARTICLE
10.1029/2025JG009611

# Effects of Wildfire on Soil Hydraulic Properties in the Western Oregon Cascades

**Cedric Pimont[1], Evan A. Thaler[2], Brian A. Ebel[3], and Kevin D. Bladon[1,2]**

[1]Department of Forest Engineering, Resources, and Management, Oregon State University, Corvallis, OR, USA, [2]Department of Forest Ecosystems and Society, Oregon State University, Corvallis, OR, USA, [3]U.S. Geological Survey, Water Resources Mission Area, Burlington, VT, USA

**Key Points:**

- Wildfire increased soil hydraulic conductivity, sorptivity, and wetting front potential but decreased water repellency
- There were no differences in soil hydraulic properties across locations impacted by different burn severity
- Soil hydraulic properties were better explained by soil physical properties than landscape attributes

**Supporting Information:**

Supporting Information may be found in the online version of this article.

**Correspondence to:**

E. A. Thaler,
thaler.evan@gmail.com

**Citation:**

Pimont, C., Thaler, E. A., Ebel, B. A., & Bladon, K. D. (2026). Effects of wildfire on soil hydraulic properties in the Western Oregon Cascades. *Journal of Geophysical Research: Biogeosciences*, *131*, e2025JG009611. https://doi.org/10.1029/2025JG009611

Received 3 DEC 2025
Accepted 25 APR 2026

**Abstract** Wildfires can substantially impact the hydrology of forested watersheds, increasing the risk of hydrologic hazards such as flash floods and debris flows. Soil hydraulic properties related to infiltration are a key control in determining the timing and magnitude of these hydrogeomorphic events. In our study, we collected 445 soil cores from burned (216 cores) and unburned (229 cores) reference catchments and analyzed them for soil hydraulic properties 10 months after the 2022 Cedar Creek Fire in Oregon, USA. We observed significantly greater field-saturated hydraulic conductivity ($K_{fs}$), sorptivity ($S$), and wetting front potential ($\Psi_f$) in burned soils relative to unburned soils, with median ratios of 5.7, 4.4, and 5.0, respectively. Among low-, moderate-, and high burn severity groups, soil hydraulic properties were not statistically different. Reductions in median soil bulk density with increasing burn severity suggested an expansion of pore sizes, which may have been partially responsible for increasing $K_{fs}$ and $S$. Additionally, in some burned soil samples, the increase in soil hydraulic properties may have been partially related to a concurrent reduction in "natural background" water repellency that is characteristic of dry, unburned soils in the Western Cascades. We observed no evidence of spatial autocorrelation in $K_{fs}$ using semivariogram analysis. Principal component analysis paired with a $k$-means cluster analysis suggested that soil physical properties explained variations in soil hydraulic properties better than landscape attributes. Although there is a lack of regional results for comparison, our results trend in the opposite direction from drier, lower net primary productivity regions that are typically studied for post-wildfire soil hydraulic properties.

**Plain Language Summary** Wildfires can increase the risk of hazards by altering the soil hydrology of watersheds, particularly in forested catchments. In this study, we compared soil hydraulics between an unburned and a burned catchment with a range of burn severities in western Oregon, USA. We found significantly greater hydraulic conductivity, sorptivity, and wetting front potential in burned soils relative to the unburned soils but found no statistically significant influence of burn severity on these soil hydraulic properties. These results contrast with studies of hydraulic properties in more arid regions, where post-fire soil hydraulic characteristics decrease relative to unburned reference sites and illustrate the need for region-specific parameterization of models of post-fire watershed hydrologic changes.

## 1. Introduction

Wildfires are part of the natural cycle of disturbances of many forested ecosystems (Agee, 1998). Mixed-severity fires help increase species diversity (Burkle et al., 2015), enhance aquatic habitat (Bisson et al., 2003), and sequester carbon long-term through the production of pyrogenic carbon (Santín et al., 2015). In recent decades, wildfires have grown in size and severity across many regions, including the western United States (US; Dennison et al., 2014; Parks et al., 2025). These trends have been linked to anthropogenic climate change leading to earlier spring snowmelt and warmer temperatures (Adams, 2013; Westerling, 2016; Westerling et al., 2006), decreased relative humidity, and increased fuel aridity (Abatzoglou & Williams, 2016). Additionally, decades of fire suppression in forests in the western US have led to increased density of fuels, as well as less fire-tolerant vegetation, which has contributed to increased occurrence of large, high-severity wildfires (Perry et al., 2011).

Wildfire can impact hydrologic processes in forests, reducing canopy interception (Williams et al., 2019) and evapotranspiration (Ma et al., 2020; Poon & Kinoshita, 2018), leading to greater net precipitation (Cardenas & Kanarek, 2014; Holden et al., 2015). Combined with greater net precipitation (Williams et al., 2019) and increased transfer of raindrop kinetic energy to the soil (Noske et al., 2022), changes in soil properties and

reductions in ground cover due to wildfire can lead to increases in erosion (Vieira et al., 2015), hillslope runoff rates (Shakesby & Doerr, 2006), altered streamflow regimes (Hallema et al., 2017), and more runoff-induced debris flows (Cannon & DeGraff, 2009; Cannon et al., 2008; Hoch et al., 2021), which increase stream sediment loads. These impacts, along with changes in stream chemistry (Beyene et al., 2021; Emelko et al., 2011; Rust et al., 2018; Smith et al., 2011), have led to concerns regarding the impacts of wildfires on water supplies for downstream community drinking water and aquatic ecosystem health (Bladon et al., 2014; Emelko et al., 2011; Nyman et al., 2021; Robinne et al., 2021).

A central control on these post-fire hydrologic responses is soil infiltration capacity (Cerdà & Robichaud, 2009; McGuire et al., 2024; Neary, 2011; Noske et al., 2016; Nyman et al., 2011; Sheridan et al., 2007, 2016; Van der Sant et al., 2018), which is governed by soil hydraulic properties including field-saturated hydraulic conductivity ($K_{fs}$), sorptivity ($S$), and wetting front potential ($\psi_f$) (Rengers et al., 2016). However, reported post-fire responses of these properties are highly variable (Neary, 2011; Nyman et al., 2014; Perkins et al., 2022). For example, hydraulic conductivity has been observed to decrease by 10%–40% following prescribed fire and wildfire (Ebel & Moody, 2017; Robichaud, 2000). In other systems, 60%–70% reductions in infiltration have been reported in burned areas relative to unburned areas (Ebel, 2019; Ebel & Moody, 2020; Larson-Nash et al., 2018), with some cases approaching near-impermeable conditions (Ebel et al., 2012). Conversely, $K_{fs}$ has remained unchanged or even increased following wildfire in environments with relatively high soil organic matter or under prescribed and laboratory burn conditions (Burgy & Scott, 1952; Chief et al., 2012; Ebel et al., 2019; Wieting et al., 2017). Although $S$ has been observed to decline linearly with burn severity and $K_{fs}$ to decline exponentially (Moody et al., 2016), these relationships often weaken during post-fire recovery (Ebel et al., 2022).

Wildfire influences soil hydraulic properties through several interacting mechanisms:

- Enhancement or reduction in soil water repellency influences capillary flow and $S$ (Ebel & Moody, 2017; Moody & Martin, 2009; Shillito et al., 2020) and can limit effective wetting during rainfall events (Nyman et al., 2014). Repellency may be enhanced (Chen et al., 2020) or reduced (Doerr et al., 2006) following fire and is highly spatially variable (Nyman et al., 2010; Weatherholt & Johnson, 2024; Woods et al., 2007), often varying with proximity to pre-fire canopy (Madsen et al., 2011).
- Combustion of organic matter and vegetation roots, which reduces aggregate stability, a measure of cohesiveness of soil particles in forming larger aggregate macrostructure (Mataix-Solera et al., 2011; Varela et al., 2015), and alters microporosity. In some soils, heating may fuse clays and increase aggregate stability (Hrelja et al., 2020), demonstrating soil-type dependence. Increases in near-surface soil bulk density, which reduce pore size and connectivity, can potentially decrease $K_{fs}$ (Ebel & Moody, 2020).
- Surface sealing and ash-induced pore clogging from raindrop impact (Larsen et al., 2009; H. Liu et al., 2011; Robichaud et al., 2016; Woods & Balfour, 2010) have effects dependent on soil texture; coarse sandy loams may be more prone to infiltration decline than finer silt loams under certain rainfall conditions (Woods & Balfour, 2010).

Because these mechanisms operate simultaneously and vary with burn severity, soil texture, vegetation type, antecedent soil moisture, and time since fire, wildfire does not impose a uniform hydraulic response across landscapes.

In addition to the effects of fire, topography can also influence soil hydraulic properties. Landscape-scale variables such as slope (Baiamonte et al., 2017; Casanova et al., 2000), aspect (Guo & Ma, 2023), and elevation (Baiamonte et al., 2017) have all been shown to explain variations in hydraulic conductivity. For example, in a Chilean catchment, areas with shallower slopes had lower hydraulic conductivity due to increased pore clogging (Casanova et al., 2000). Additionally, aspect-wildfire interactions have been demonstrated to alter soil moisture dynamics in the Colorado Front range (Ebel, 2013), which may have an influence on temporal changes in infiltration, as soil moisture is an important factor for water repellency persistence and vegetation recovery (Huffman et al., 2001; Noske et al., 2016; Perkins et al., 2022; Van der Sant et al., 2018).

Spatial scaling of hydraulic conductivity is challenging, as point scale measurements are often poorly related to catchment scale estimations of hydraulic conductivity in post-fire watersheds (Hoch et al., 2021; Langhans et al., 2016; Liu et al., 2023; McGuire et al., 2018). Poor scaling may often be due to measurements covering only a small, easily accessible portion of the watershed which they are intended to represent. Quantifying the spatial variability of soil hydraulic properties across a catchment is important for understanding watershed responses to

precipitation, and allows for a more nuanced approach to watershed modeling for improved prediction of rainfall-runoff responses (Ebel et al., 2016; McGuire et al., 2018; dos Santos et al., 2021). Although previous research has attempted to use topography to predict soil hydraulic properties (Leij et al., 2004), the interactions between wildfire, topography (i.e., elevation, slope, aspect, topographic position), and soil hydraulic properties have not previously been investigated in regions with a Mediterranean climate impacted by infrequent, high severity wildfires, such as the western Cascade Range of the Pacific Northwest.

Soil hydraulic properties, particularly $K_{fs}$, are important parameters for numerical modeling of watersheds (Borah, 2011). However, there is little information on how soil hydraulic properties vary due to the complex interactions of wildfire and topography. Additionally, there appears to be no published data on post-fire soil hydraulic properties for the Western Cascades region of Oregon, USA, which is a region that has observed several large, high severity wildfires in recent years. In our study, we addressed the following questions using spatially distributed measurements of infiltration.

1. How do soil hydraulic properties differ between unburned and burned watersheds in the western Cascade Range of Oregon?
2. Across burned and unburned catchments, can soil hydraulic properties be explained by (a) burn severity, (b) catchment topography (slope, aspect, elevation, Topographic Position Index), (c) soil physical properties (texture, organic matter (OM) content), and (d) antecedent soil moisture content?

## 2. Materials and Methods

### 2.1. Study Area

The Cedar Creek Fire burned more than 51,000 ha in the Middle Fork Willamette River watershed in the central Cascade Range of Oregon in 2022 (Figure 1). The fire began on August 1st as a result of multiple lightning strikes in the Willamette National Forest and remained active until November 2022. Within the fire perimeter, 15% of the area was classified by the Monitoring Trends in Burn Severity (MTBS) program (Eidenshink et al., 2007) as high burn severity, 21% as moderate severity, 31% as low severity, and 32% as unburned. The burn area was upstream of two reservoirs, Lookout Point Lake and Dexter Reservoir, which are used to produce electricity and provide flood control for the region.

For our study of the Cedar Creek Fire, we selected Infestation Creek (50 ha; 43.7777602°N, 122.3006375°W; Figure 1) as our burned catchment and False Berry Creek (46 ha; 43.6352781°N, 122.3187104°W; Figure 1) as our unburned reference catchment. The Infestation Creek catchment was 100% burned at mixed severity. Our two study catchments had similar slopes, aspects, elevations, geology, and vegetation types to facilitate comparisons and isolate the effects of wildfire (Table 1).

The regional climate is Mediterranean (Köppen: Csb (Peel et al., 2007), with cold, wet winters and warm, dry summers. Annual average precipitation is 1,800 mm with a mix of rain and snow, with snow and overall precipitation increasing with elevation. Approximately half of this precipitation falls between the months of December and February, whereas minor amounts (~40 mm) fall in the summer. The 30-year mean daily air temperatures have been ~7°C with mean daily maximum temperatures reaching only 4.5°C in January but 25°C in July (Daly et al., 1997). Pre-fire overstory vegetation consisted primarily of Douglas-fir (*Pseudotsuga menziesii*), western hemlock (*Tsuga heterophylla*), and western red cedar (*Thuja plicata*), with bigleaf maple (*Acer macrophyllum*) and red alder (*Alnus rubra*) in riparian areas. Understory vegetation comprised largely of Oregon grape (*Berberis aquifolium*), salal (*Gaultheria shallon*), sword fern (Sp. *munitum*), vine maple (*Acer circinatum*), and Pacific rhododendron (*Rhododendron macrophyllum*) with manzanita (*Arctostaphylos manzanita*) and Pacific poison-oak (*Toxicodendron diversilobum*) in small areas. The geology is composed largely of basaltic and andesitic rocks of the Little Butte Volcanics (Mineral Resources Online Spatial Data: Geologic Maps, 2023). Soils in both the Infestation Creek and False Berry Creek watersheds are mapped as gravelly silt loams with layers of volcanic ash present in the uppermost layers (Soil Survey Staff, Natural Resources Conservation Service, 2026).

### 2.2. Study Design

Soil cores were collected from the burned and unburned watersheds approximately 1-year post-fire (July–September 2023) using a 5.1-cm diameter by 8-cm long steel sampling ring. Within each watershed, we collected an

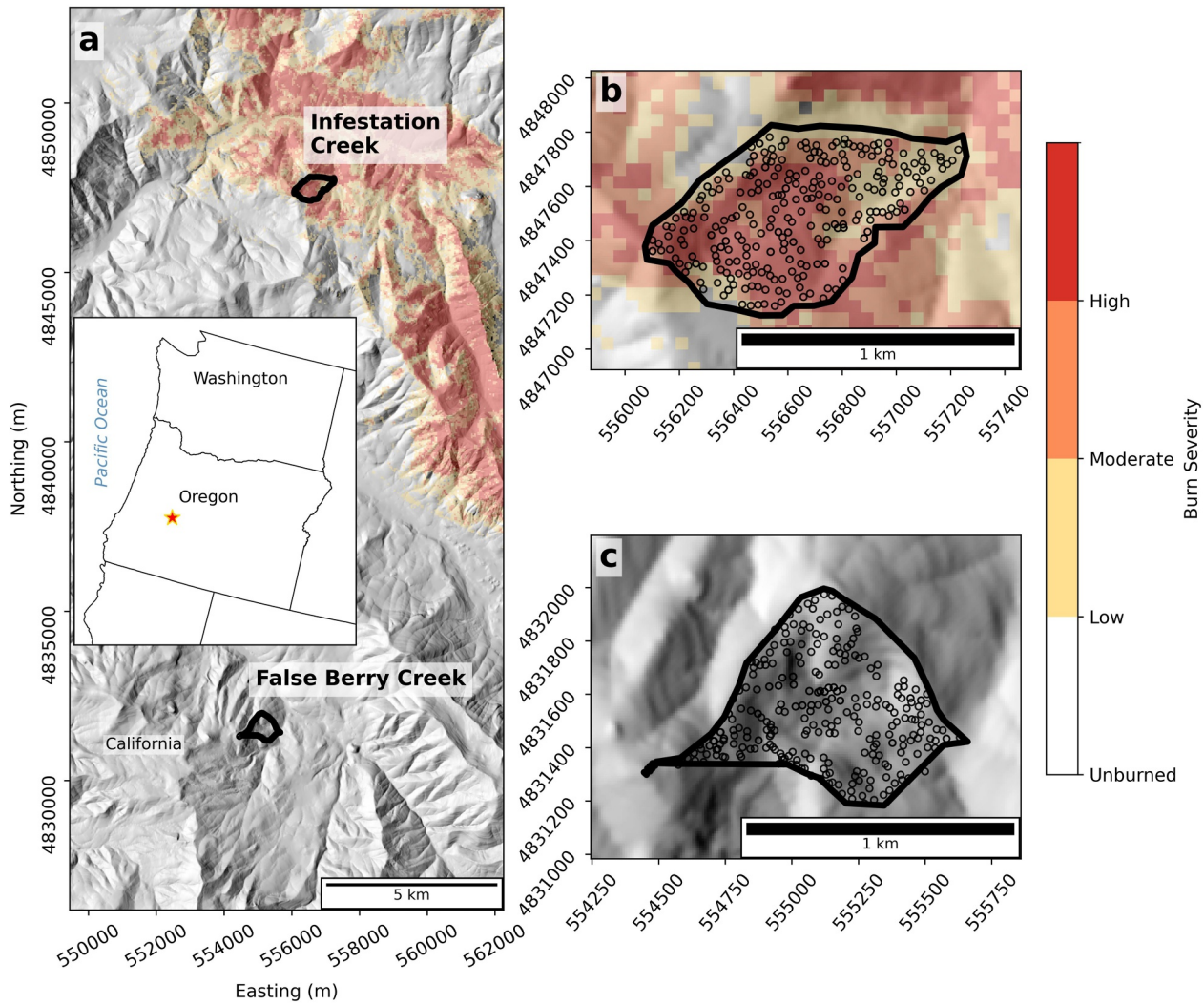


**Figure 1.** Maps of the study watersheds. (a) Location of Infestation Creek within the Cedar Creek Fire and False Berry Creek the paired unburned watershed within the state of Oregon, USA (inset map). (b) Soil sampling locations (black circles) and burn severity map of the Cedar Creek Fire within the Infestation Creek watershed, and (c) soil sampling locations in the unburned False Berry Creek watershed. Map coordinates are NAD83 UTM Zone 10.

even spatial distribution of soil cores, which were kept intact in storage prior to laboratory analysis. Sample locations were evenly distributed spatially, using randomly generated points, across the entire area of both Infestation Creek (burned; 216 soil samples) and False Berry Creek (unburned, reference; 229 soil samples) watersheds.

Sampling points were predetermined using the Create Random Points tool in ArcGIS Pro (Esri, Redlands, CA, USA) with an arbitrarily selected minimum 15 m distance between points. If we could not physically reach a sample point or easily sample the surface mineral soil due to the presence of rocks, we shifted the point to a nearby alternate location. At each soil sample location, we quantified the litter depth with a ruler. We also recorded the

**Table 1**
*Topographic Characteristics of Our Two Study Watersheds, Infestation Creek (Burned) and False Berry Creek (Unburned, Reference)*

| Watershed | Area (ha) | Mean dNBR [range] | Mean catchment slope (degrees) [SD] | Mean aspect (degrees) | Mean TPI | Mean elevation (m) [range] |
|---|---|---|---|---|---|---|
| Infestation Creek | 50 | 721 [42–1,155] | 22.2 [6.3] | 80 | 0.47 | 959 [729–1,186] |
| False Berry Creek | 46 | 0 [0-0] | 25.85 [8.3] | 111 | 0.20 | 865 [721–1,128] |

*Note.* The dNBR (Key & Benson, 2005) is the change in the normalized burn ratio. TPI is Topographic Position Index, and SD is standard deviation.


**Figure 2.** Examples of (a) collecting a soil core in the burned area, (b) a high severity burned hillslope (~1,000 dNBR), (c) organic duff layer removal in preparation for collecting a soil sample in an unburned area, and (d) vegetation in the unburned area including Douglas-fir (*Pseudotsuga menziesii*), Pacific rhododendron (*Rhododendron macrophyllum*), and vine maple (*Acer circinatum*).

Global Positioning System coordinates of each sample location to sub-meter accuracy using a Trimble DA2 GNSS receiver (Trimble Inc., Westminster, CO, USA).

Where present, the litter and duff layer was removed from the soil surface prior to collecting the soil sample (Figure 2), as we assumed that coarse organic material would not limit infiltration rates and would interfere with Mini Disk infiltrometer measurements. A thin layer of petroleum jelly was applied to the inside of each soil sampling ring prior to collecting the soil sample to reduce preferential flow along the core wall during laboratory infiltration measurements. The sampling rings were inserted into the ground using a metal driving/hammering head (Figure 2). When necessary, we used a mallet to tap on the driving head to insert the soil sampling ring due to dry conditions and fine texture of the soil. After extraction of the sampling ring and soil core, both ends of the cores were sealed with plastic caps and electrical tape and placed in a cooler with ice packs. Samples were stored in a freezer (−10°C) upon return to the laboratory until they were processed.

### 2.3. Soil Hydraulic Properties

In the laboratory, we quantified soil hydraulic properties from each soil core using a Mini Disk Tension Infiltrometer (METER group, Pullman, WA, USA) with a suction value of −1.0 cm, which represented near-saturated conditions at our site. We used a single, constant tension to ensure that all cores were evaluated under identical

hydraulic conditions, to enable cross-sample comparability. A cover of cheesecloth and a paper towel were placed under the base of the core, which was then placed in a milled stand with a hole in the bottom. An angled mirror underneath the stand provided a view of the base of the core to enable us to stop our measurements when we observed water breakthrough from the bottom of the sample. Prior to placing the infiltrometer on the sample, any rocks or large pieces of organic material were removed from the surface, which was then leveled with a scoopula to ensure full, even contact with the porous metal plate. The Mini Disk was held to the core with a clamp stand to ensure that it remained in place throughout the duration of the measurements. Water level measurements were read at 1 s intervals with an Arduino Uno R3 (Arduino Core Team) microcontroller connected to a TI FDC1004 Capacitance to Digital converter chip (Texas Instruments, Inc, Dallas, TX, USA). The chip was connected to two strips of parallel copper tape, which ran the length of the reservoir chamber in the Mini Disk. The chip measured the capacitance of the tapes and therefore functioned as an electrode. In this case, the change in capacitance was linearly proportional to the change in water level, so we converted the change in capacitance to infiltrated volume using the coefficient derived from calibration runs on practice cores. The method was not sensitive to bubble formation within the Mini Disk tube, unlike previously used differential pressure transducer methods (Moody et al., 2019). However, it was prone to external interference from nearby foreign objects such as cell phones and human hands. Because of occasional drift in output capacitance, if there was significant variability or errors in the measurements, we returned the core to the refrigerator and allowed it to air dry until it reached the initial mass prior to re-running the sample. When the soil surface was too irregular or coarse to interface properly with the infiltrometer's porous plate, we applied a fine layer of coarse contact sand (~1 mm) to the soil surface. In these cases, we weighed the sand applied to enable us to correct for it in measurements of water content and bulk density.

Because our soil sample cores had a similar diameter to the porous plate of the Mini Disk, infiltration into the sample was assumed to be one-dimensional. The total infiltrated volume with time for each sample was fitted with the three curve-fitting methods (Vandervaere et al., 2000a). These included the cumulative infiltration method (Equation 1), cumulative linearization method (Equation 2), and the differentiated linearization method (Equation 3):

$$I = S\sqrt{t} + C_2 t, \tag{1}$$

$$\frac{I}{\sqrt{t}} = S + C_2\sqrt{t}, \tag{2}$$

$$\frac{dI}{d\sqrt{t}} = S + 2C_2\sqrt{t} \tag{3}$$

where $I$ is the cumulative infiltration depth in mm, $S$ in mm hr$^{-1/2}$, $t$ is time in seconds, and $C_2$ is the coefficient proportional to the $K_{\mathrm{fs}}$ in mm hr$^{-1}$. The coefficients for all three methods were averaged (excluding negative values) similar to (McGuire et al., 2018). $K_{\mathrm{fs}}$ was obtained from $C_2$ with the following equation outlined in (Vandervaere et al., 2000a):

$$K_{\mathrm{fs}} = \frac{3C_2}{2-\beta}. \tag{4}$$

The shape constant coefficient, $\beta$, ranges from 0 to 1, but as it is unknown, it was set to 0.6, which assumed lognormally distributed error (Vandervaere et al., 2000b). Once $S$ and $K_{\mathrm{fs}}$ were estimated, we calculated the soil wetting front potential ($\Psi_f$) with Equation 5 (White & Sully, 1987):

$$\Psi_f = \frac{S^2}{2(\theta_s - \theta_i)K_{\mathrm{fs}}} \tag{5}$$

where $\theta_s$ is the saturated water content and $\theta_i$ is the initial water content. We assumed $\theta_s$ to be equivalent to porosity, which can be approximated from bulk density with the equation:

$$\theta_s = 1 - \frac{D_b}{\rho_s} \quad (6)$$

$\rho_s$ is the density of solids, which we estimated by measuring saturated water content for 10 burned and 10 unburned samples rather than using the typical 2.65 g $cm^{-3}$ for quartz due to the high organic matter content and volcanic origin of our soil samples. To saturate our soil samples, the sample cores were placed in water with cheesecloth over the ends and allowed to saturate. Samples were considered saturated when contiguous weight measurements, separated by 24 hr, were the same. We then emptied the samples into aluminum tins and oven dried these samples at 105°C for 24 hr to measure the bulk density ($D_b$). We fit a linear regression to Equation 6 between $\theta_s$ and $D_b$ with $\rho_s$ as the unknown coefficient that was assumed to be constant for all samples.

Although recent studies have indicated that the standard experimental measurement methods can produce bias in absolute values of soil hydraulic properties (Gerke et al., 2026; Khirevich et al., 2022), our measurements of both the unburned (reference) and burned samples followed the same protocols. Hence, the bias introduced from the experimental methods does not preclude assessment of the relative difference between the unburned and burned soils, which was the primary focus of our study.

### 2.4. Supporting Soils Data

To quantify the antecedent water content, we weighed our soil samples prior to quantifying the soil hydraulic properties. We weighed the samples again after they were oven dried at 105°C for 12–24 hr. Following the infiltration tests, the gravimetric water content (ω) was calculated by subtracting the oven dried mass from the initial mass of the wet soil and then dividing that difference by the wet mass. We also estimated dry bulk density by dividing the oven dried mass by the core volume (163.4 $cm^3$). The initial volumetric water content ($\theta_i$) was then estimated by multiplying the gravimetric water content by bulk density, with an assumed density of 1 g $cm^{-3}$ for water.

$$\theta_i = \omega D_b \quad (7)$$

From each soil core, we quantified organic matter content using the loss on ignition method (Hoogsteen et al., 2015). We placed two subsamples of soil (1–3 g) from the top 0–2 cm of each soil core in ceramic crucibles. The samples were then weighed and transferred to a muffle furnace where they were heated at 550°C for 3 hr. Samples were then cooled in a desiccator and weighed again. Samples with applied contact sand were excluded in the analysis of surface organic matter content.

We quantified soil texture on all 445 soil samples with a Bettersizer 2600 laser diffraction particle analyzer (Bettersize Instruments Ltd.) using a 1 g sample from the middle 2–5 cm of the core. Organic matter was removed prior to insertion into the machine using 6% sodium hypochlorite adjusted to a pH of 9.5 (Heckman et al., 2009; Mikutta et al., 2005). Sample solutions were placed in a hot water bath (95°C–100°C) for 15 min and then centrifuged for 5 min at 3,500 rotations per minute. The supernatant was poured off after centrifuging, leaving behind mineral soil. We repeated this process until the supernatant turned pink, indicating organic matter removal (typically 2–3 rounds).

### 2.5. Topographic Data

We analyzed the spatial data layers of our study catchments from a 1 m resolution, LiDAR-derived Digital Elevation Model (DEM) using tools in ArcGIS Pro. Slope and aspect were derived directly from the DEM using Esri's respective tools. Topographic Position Index (TPI) is a unitless geospatial parameter describing slope position and landform type (Weiss, 2001) and may also be an important predictor of soil properties. Neighborhood distance is an important metric when calculating TPI, with larger neighborhood distances (>1,000 m) suited for classifying landforms at the basin scale, and small neighborhood distances (<100 m) more appropriate for the hillslope scale. Given the scale and spatial resolution of the samples and measurements we made in our study, we used a 100 m neighborhood distance. TPI was calculated by subtracting the mean neighborhood elevation from the original DEM. Finally, the values were normalized by calculating the standard deviation of each cell relative to a mean of 0. Negative TPI values represent lower slope and valley bottom positions, whereas positive values

are associated with upper slope and ridgetop areas. We also calculated the "northness" of aspect, how close the aspect of each cell was to being north-facing, from the traditional 360° aspect using the formula:

$$\text{northness} = \frac{\text{abs}(\text{Aspect} - 180)}{180} \quad (8)$$

Northness values range from 0 to one, where 0 indicates the most south-facing slopes and 1 indicates the most north-facing slopes, which creates a continuous variable that is useful for model inputs. In addition to DEM-based layers, a layer of thematic burn severity obtained from MTBS provided a categorical metric of immediate post-fire burn severity.

### 2.6. Statistical Analysis

$K_{fs}$ values typically follow a log-normal distribution (Feng & Vardanega, 2019; Talsma & Hallam, 1980; Wilson et al., 1989) while $S$ values are usually normally distributed. We used the nonparametric Mann-Whitney signed-rank test to examine statistical differences in the soil hydraulic properties between the burned and unburned soils. $P$-values from post hoc tests for differences between burn severity groups were adjusted using Bonferroni correction. To evaluate controls on soil hydraulic properties, we first conducted principal component analysis (PCA) on all of the soil hydraulic, physical, and topographic variables. Prior to performing the PCA, the data were scaled using z-score standardization. Following the PCA, we applied $k$-means clustering to the two most important principal components derived from the PCA. We used the average silhouette (Kaufman & Rousseeuw, 2009) and gap statistic (Tibshirani et al., 2001) methods to determine the optimal number of clusters. The stabilities of the clusters were determined using the Jaccard similarity coefficient ($J$) (Hennig, 2007); clusters with $J \geq 0.75$ are considered stable. We assessed differences in soil hydraulic properties and supporting variables between the groups using the non-parametric Kruskal-Wallis test, and when the Kruskal-Wallis test indicated statistically significant differences between unburned and burned (including low, moderate, and high severity) groups ($p < 0.05$), we used the post hoc Dunn's test to compare pairwise differences between the subgroups. The Ansari-Bradley test was used to compare the scale parameters (variance of the distributions) for soil hydraulic properties in the burned and unburned sites. Semivariogram results suggested no spatial covariance in soil hydraulic properties, so all samples were treated as independent (Figure S1 in Supporting Information S1).

## 3. Results

### 3.1. Hydraulic Properties of Burned and Unburned Soils

Overall, we found a strong effect of wildfire on infiltration-related soil hydraulic properties. Field-saturated hydraulic conductivity ($K_{fs}$) had a median value of 21.7 mm hr$^{-1}$ (95% CI: 15.1–31.8 mm hr$^{-1}$) in unburned soils and 123.2 mm hr$^{-1}$ (95% CI: 86.9–158.8 mm hr$^{-1}$) in burned soils (Mann-Whitney (M-W) U test, $W = 17{,}317$, $p < 0.001$). Post hoc Dunn's tests indicated that the low, moderate, and high severity burn sites were statistically indistinct, while the unburned sites were statistically lower than each of the burn severity groups (Figure 3). Estimates of $K_{fs}$ were highly variable and spanned multiple orders of magnitude in both burned and unburned soils (Figures 3a and 4; Tables S1 and S2 in Supporting Information S1). However, despite the differences in medians and geometric means, there was limited statistical evidence for differences in the variability in $K_{fs}$ (estimated by scale parameters corresponding to the shape of the distributions) between burned and unburned sites (Ansari-Bradley (A-B) test, AB = 25,127, $p = 0.045$).

$S$ had a median value of 1.9 mm hr$^{-1/2}$ (95% CI: 1.4–2.4 mm hr$^{-1/2}$) in unburned soils and 8.4 mm hr$^{-1/2}$ (95% CI: 6.4–12.8 mm hr$^{-1/2}$) in burned soils. $S$ was statistically greater in burned soils (M-W, $W = 14{,}161$, $p < 0.001$), where the ratio of geometric means for $S$ (burned/unburned) was 3.77 (Figure 3). The post hoc Dunn's test indicated that $S$ was similar between the low-, moderate-, and high severity burned sites, whereas the unburned sites were statistically lower than each of the burned severity groups (Figure 3b). Unlike $K_{fs}$, the scale parameter for $S$ was significantly greater in soil samples from the burned sites compared to unburned sites (A-B, AB = 23,382, $p < 0.001$), indicating a wider distribution of values in the burned soil samples.

For the Green-Ampt wetting front potential ($\Psi_f$), we observed a median value of 0.25 mm (95% CI: 0.13–0.47 mm) in unburned soils and of 1.26 mm (95% CI: 0.77–1.89 mm) in burned soils (M-W, $W = 19{,}576$, $p < 0.001$). Post hoc Dunn's tests indicated that $\Psi_f$ was similar between the unburned, low, and moderate severity

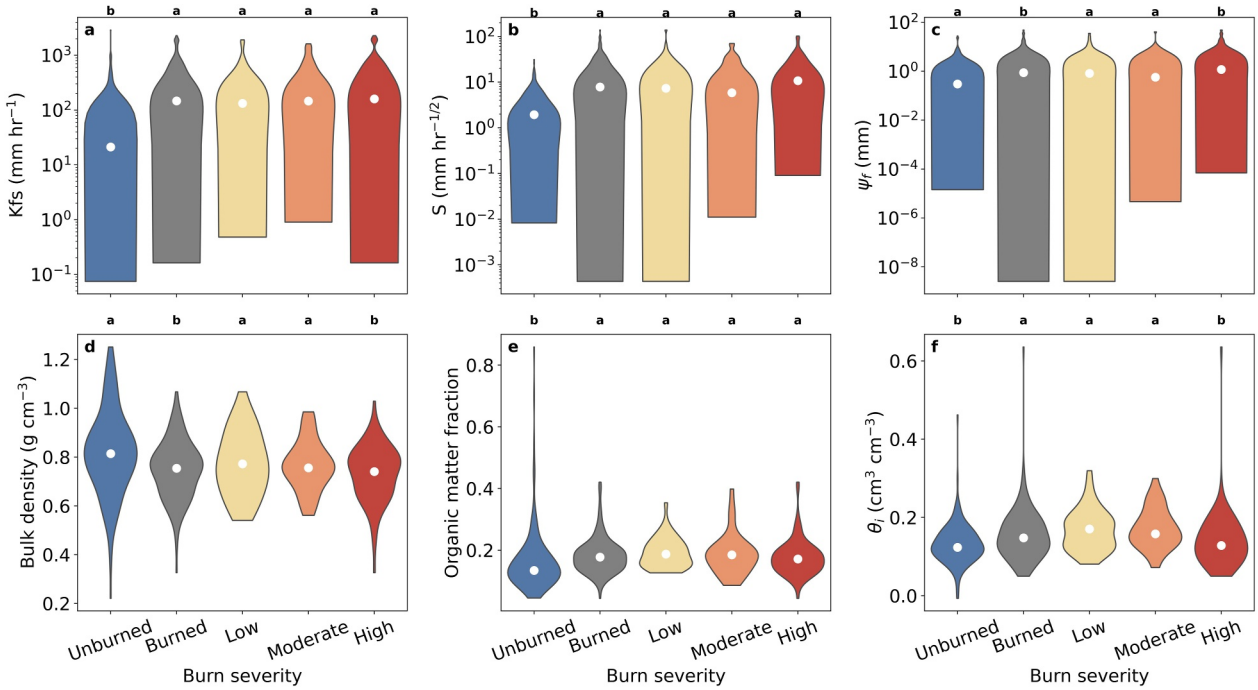


**Figure 3.** Violin plots of (a–c) soil hydraulic properties and (d–f) soil physical properties in the unburned (blue) and burned (gray) catchments. Soil properties in the burned catchments are further divided into burn severity classes low (yellow), moderate (orange), and high (red). Letters on the top axis of each plot represent statistically similar groups.

burned sites, whereas the grouped burned sites and high burn severity sites were statistically greater (Figure 3c). The variability in $\Psi_f$ was also greater in the burned soils compared to the unburned soils, indicated by a significant difference in scale parameters (A-B, AB = 24,570, $p = 0.003$).

### 3.2. Soil Physical Properties

The majority of our soil samples, regardless of burn severity, were classified as having silt loam texture (Figure 4a). However, the mean clay content was 20.2 ± 5.4% (95% CI: 19.4%–21.0%) in the unburned soils and 14.7 ± 5.1% (95% CI: 14.0%–15.6%) in the burned soils. The clay content was statistically different between the burned and unburned soils (two-sample $t_{df\ =\ 352.01} = 9.8$, $p < 0.001$). Burn severity was a significant factor in explaining variations in clay content (ANOVA, $F = 35.96$, $p < 0.001$), with unburned samples having the highest mean clay content 20.2 ± 5.4% compared to 15.8 ± 5.0%, 16.5 ± 6.3%, and 13.7 ± 4.4% in soils from low-, moderate-, and high burn severity sites, respectively (Figure 4b). The clay content was significantly different between the unburned soils and both the low and high burn severities ($p$-adj < 0.001, difference = 2.1 ± 2.5%, 6.5 ± 1.7%). Clay content was significantly greater in the unburned soils than in the soils from moderate burn severity sites ($p$-adj < 0.001, difference = 3.7 ± 2.5%), which was greater than soils in the high burn severity sites ($p$-adj = 0.039, difference = 2.8 ± 2.7%). However, clay content in soils that burned at low and high burn severity were not statistically different ($p$-adj < 0.112, difference = 2.1 ± 2.7%).

Overall, bulk density ($D_b$) was relatively low, which is typical of soils of volcanic origin with high organic matter content (Nanzyo et al., 1993). However, $D_b$ was lower in burned soil than in unburned soil. Mean $D_b$ was 0.83 ± 0.17 g cm$^{-3}$ (95% CI: 0.80–0.85 g cm$^{-3}$) for unburned soils and 0.74 ± 0.13 (SD) g cm$^{-3}$ (95% CI: 0.73–0.76 g cm$^{-3}$) for burned soils. $D_b$ was statistically different between the burned and unburned soils (two-sample $t_{df\ =\ 364.52}$, $t = 5.7095$, $p < 0.001$). When comparing thematic burn severity groups (Figure 3d), unburned soils had the greatest average $D_b$ at 0.83 g cm$^{-3}$, while high burn severity samples had the lowest at 0.73 g cm$^{-3}$. $D_b$ was significantly different among groups (ANOVA, $F = 11.59$, $p < 0.001$). However, there was no significant difference among burn severity groups, despite higher medians in low- and moderate severity groups relative to high severity (Figure 3d).

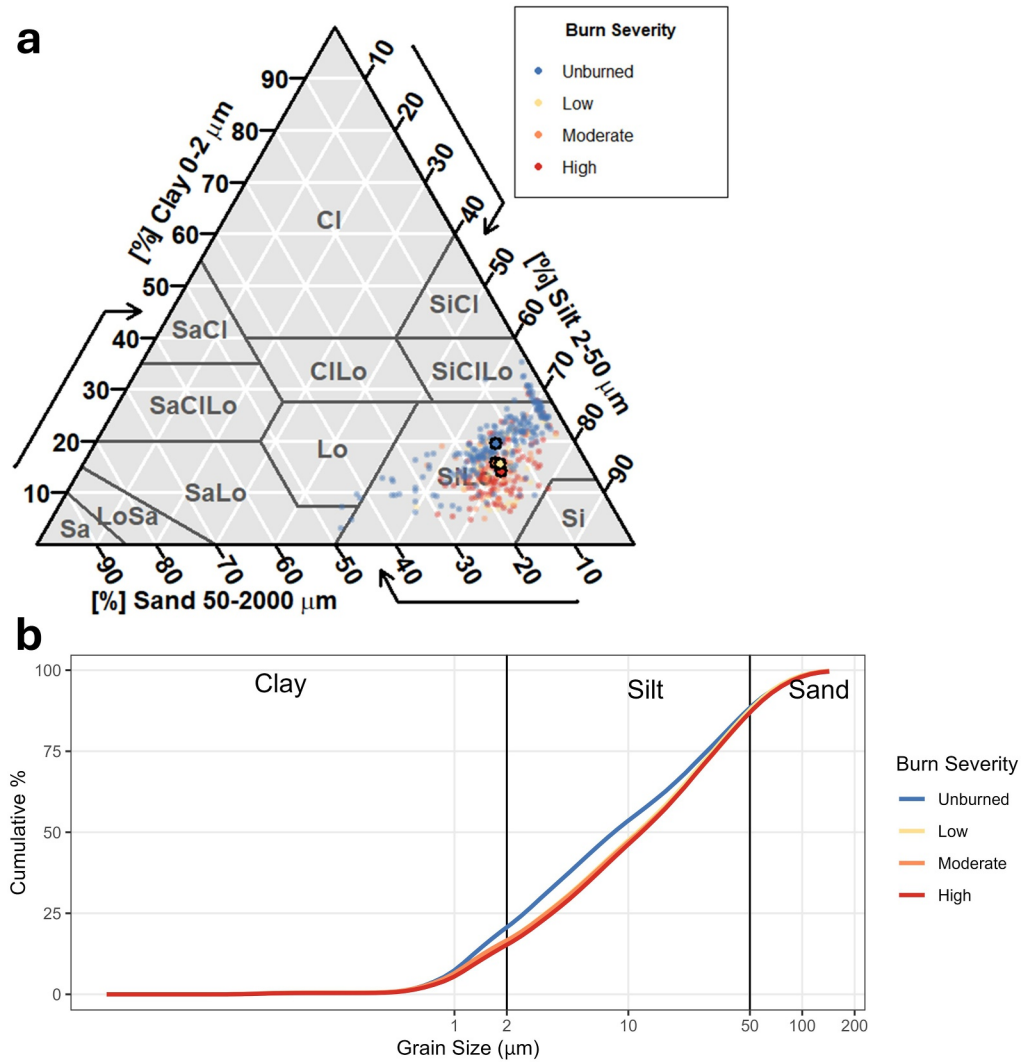


**Figure 4.** (a) USDA soil texture triangle showing sand, silt, and clay percentages of individual samples (background points) and group means (large, outlined points) and (b) mean cumulative grain size distribution curves in each burn severity group.

Mean loss on ignition (LOI) organic matter was significantly different between unburned and burned soils (two-sample $t_{df\ =\ 393.21} = 4.3852$, $p < 0.001$), with values of 15.1 ± 6.6% (95% CI: 14.2%–16.0%) and 17.8 ± 5.6% (95% CI: 17.0%–18.6%) in unburned and burned soils, respectively. The unburned samples had the lowest mean LOI values at 15.1%, whereas low severity samples had the greatest at 18.7%. Unburned soils were statistically different from low and high burn severities, whereas moderate severity LOI was not statistically different from any other group (Figure 3e).

Initial volumetric water content in our soil samples ranged from ~0–0.64 $cm^3\ cm^{-3}$, with a mean of 0.14 ± 0.06 $cm^3\ cm^{-3}$ across all samples. The mean volumetric water content was 0.14 ± 0.05 $cm^3\ cm^{-3}$ (95% CI: 0.13–0.14 $cm^3\ cm^{-3}$) in the unburned soil samples, whereas in the burned samples it was 0.15 ± 0.05 $cm^3\ cm^{-3}$ (95% CI: 0.14–0.16 $cm^3\ cm^{-3}$). Initial water contents were also different between the thematic burn severity groups (ANOVA, $F = 7.344$, $p < 0.001$). However, as evidenced by post hoc comparisons, this difference stems from differences between unburned and low/moderate severity soils (Figure 3f), whereas unburned and high severity soils did not differ statistically.

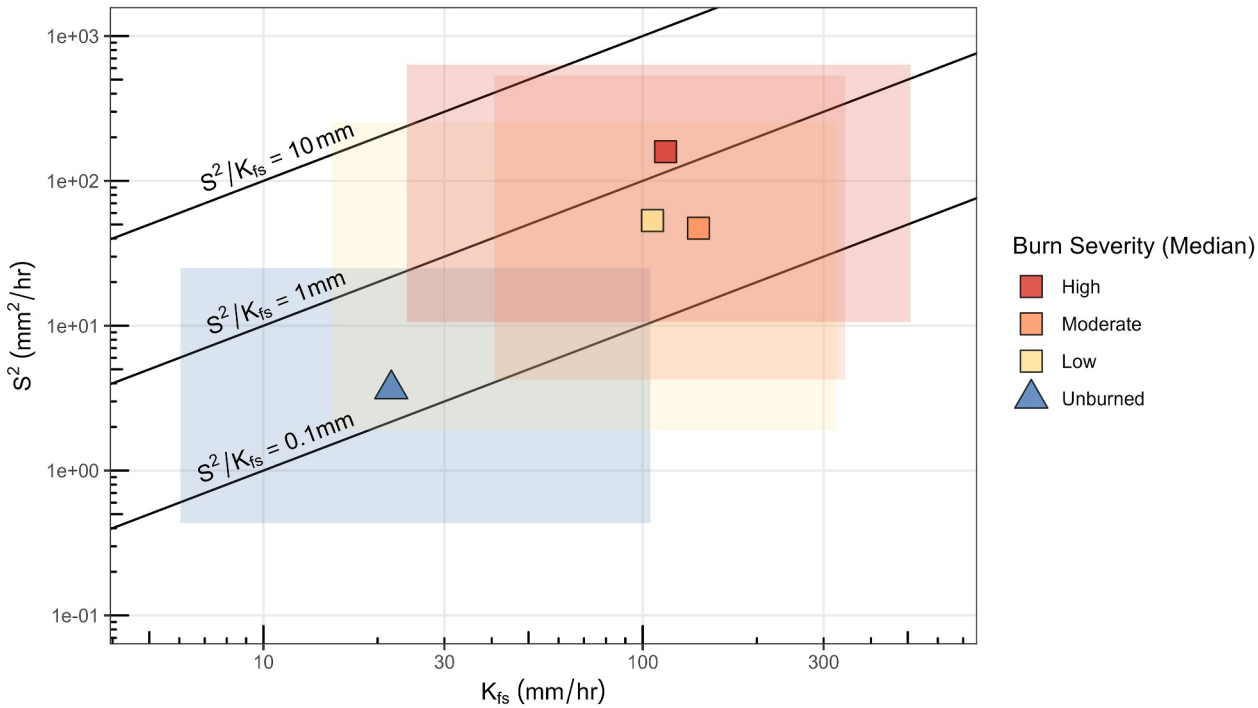


**Figure 5.** Scatterplot of field-saturated hydraulic conductivity ($K_{fs}$) versus sorptivity squared ($S^2$) by burn severity group. Light boxes are bounded by outer quartiles and solid shapes represent group medians.

### 3.3. Drivers of Soil Hydraulic Properties

Although median values of $K_{fs}$ and $S^2$ in the soils from the unburned sites had the lowest infiltration capacity, burned sites tended to group together regardless of burn severity (Figure 5). The geometric mean of $S^2/K_{fs}$ indicated an increasing trend with burn severity, from 0.13 mm in the soil samples from the unburned sites to 0.25, 0.33, and 0.93 mm in the low, moderate, and high burn severity soils, respectively. The shaded envelopes indicate that the burned watersheds occupy a broader and generally higher range of both S and $K_{fs}$ compared to the unburned watersheds.

Principal component analysis (Figure 6a) vectors indicated that $S$ and $K_{fs}$ were strongly and positively correlated with each other. Catchment-scale elevation, organic matter content (OM), and sand content were also positively correlated with $S$ and $K_{fs}$. Comparatively, clay content and bulk density were both negatively correlated with the soil hydraulic properties. We used the average silhouette and gap statistic methods to evaluate the appropriateness of our cluster analysis, with both methods indicating that a $k$ of 2 was the optimal number of clusters. The average Jaccard similarity index for both clusters using bootstrapping with replacement, jittering, and random noise was 0.90, indicating highly stable clusters. Additionally, the clusters did not overlap visually (Figure 6b). 29 unburned and 116 burned samples comprised cluster 1, while cluster 2 was composed of 145 unburned and 54 burned samples for a total of 199.

Statistical analysis of the two clusters provided strong evidence that the soil hydraulic properties ($K_{fs}$ and $S$) were both different between the two clusters, with greater values for both $K_{fs}$ (Kruskal-Wallis (K-W), H = 51.487, $p < 0.001$) and $S$ (K-W, H = 40.125, $p < 0.001$) in cluster 1 relative to cluster 2 (Figure 7). Cluster 1 also had significantly lower clay percentage and bulk density, greater sand and organic matter contents, and sites tended to have a greater elevation. Although initial water content ($\theta_i$) was significantly different between burned and unburned samples, it was not statistically different between clusters. Cluster analysis indicated that soil hydraulic properties were related to soil physical properties, and all topographic variables were significantly different between clusters; however, northness and TPI had interquartile ranges in cluster 2 that were within that of cluster 1.

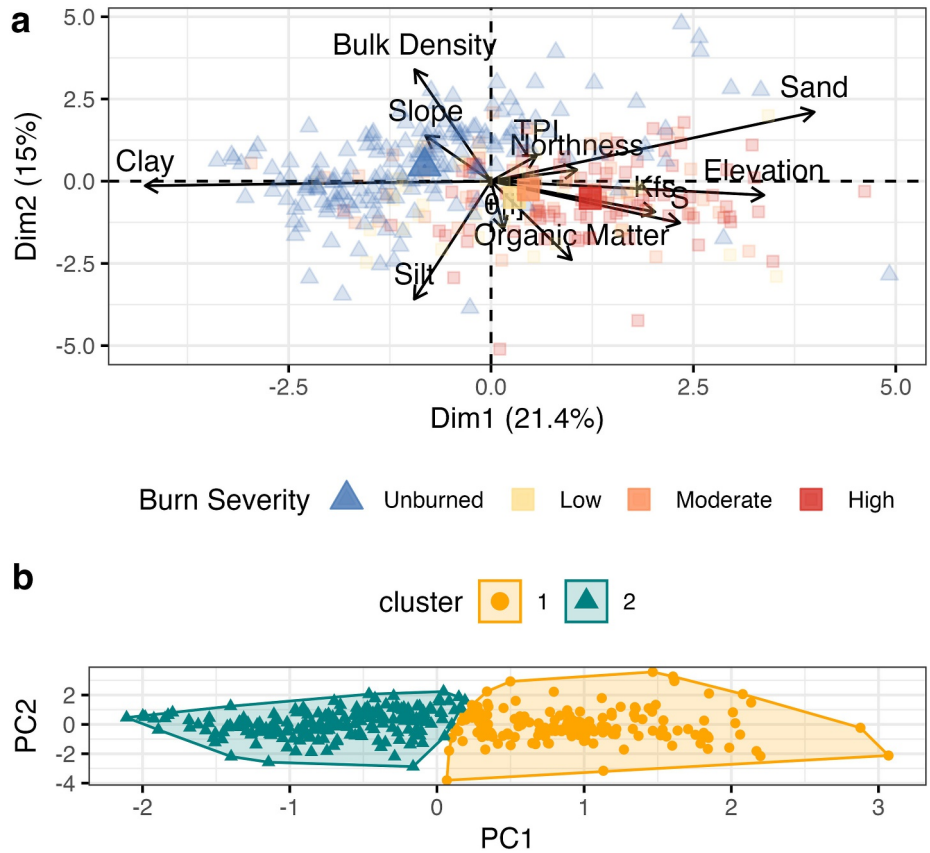


**Figure 6.** Multivariate structure of watershed soil and site characteristics across burn severity gradients. (a) Principal component analysis (PCA) biplot showing relationships among environmental variables and sampling sites colored by burn severity. Arrows represent the direction and strength of variable loadings on the first two principal components. (b) *k*-means clustering of samples in PCA space clustered by similarity in soil and topographic attributes.

We also analyzed the soil hydraulic and physical properties within each cluster. Within cluster 1 ((K-W, H = 8.9, $p = 0.0029$) and cluster 2 (K-W, H = 5.3, $p = 0.0216$), $K_{fs}$ was statistically different between burned and unburned samples. $S$ was statistically greater in the burned samples compared to the unburned samples within both clusters (Figure 8). Elevation, clay, silt, and organic matter were all different between burned and unburned soils in cluster 1, while slope, sand, bulk density, and initial water content were different in cluster 2. Analysis of between-cluster differences, isolating burned and unburned samples (Figure 8), showed they followed a similar pattern to the analysis of overall cluster differences, with some exceptions. For the unburned samples, bulk density was statistically similar between clusters (K-W, H = 0.44, $p = 0.5091$), while silt was not (K-W, H = 41, $p < 0.005$). By contrast, burned samples did have statistical differences in $S$ (K-W, H = 20, $p < 0.005$), which was lower in cluster 2, and bulk density, which was higher in cluster 2 (K-W, H = 5.4, $p = 0.0504$), but not northness or clay. Neither of the aforementioned differences was present in unburned samples.

## 4. Discussion

### 4.1. Wildfire Effects on Soil Hydraulic and Physical Properties

Contrary to previous observations, which found decreasing values of $K_{fs}$ (Moody et al., 2016), S, and $\psi_f$ (Ebel & Moody, 2017) with increasing burn severity, the soil hydraulic properties were all greater in burned soils than in unburned soils from our sites in the Western Oregon Cascades. The median $K_{fs}$ was 5.7-times greater in burned soils than the median $K_{fs}$ in unburned soils. Similarly, the ratio of burned to unburned $S$ was 4.4-times greater, and $\psi_f$ was 4.8-times greater in the burned soils. The increase in $K_{fs}$ may have been partially a result of lower bulk density ($D_b$) in the burned soils. The lower $D_b$, along with a slight increase in the proportion of silt, and a substantially lower clay content in the burned soils, indicated a potential increase in pore sizes in the burned sites,

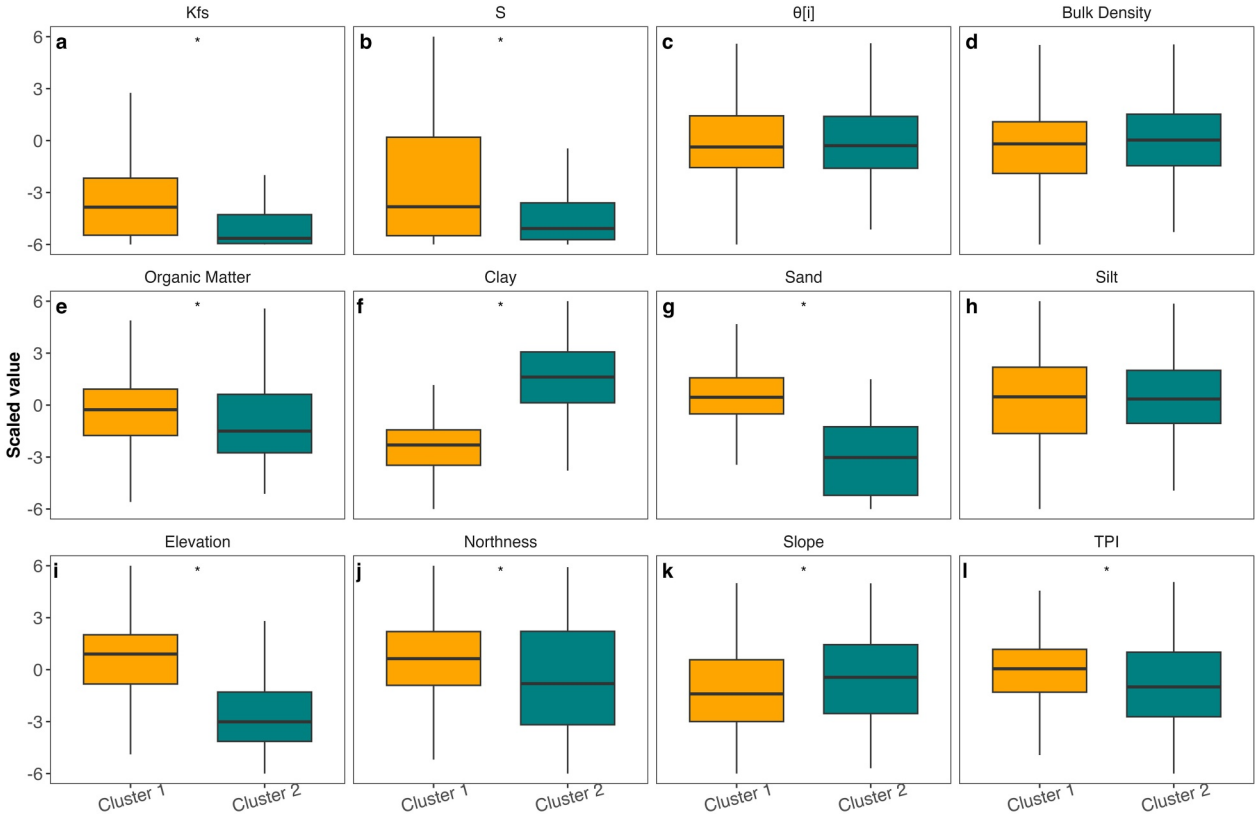


**Figure 7.** Boxplots of scaled (a–c) soil hydraulic, (d–h) soil physical, and (i–l) topographic properties in each cluster derived from *k*-means clustering analysis. Asterisks over boxplots represent significant differences between clusters at the $p < 0.05$ level using Dunn's post hoc test.

which could have contributed to the elevated $K_{fs}$ (Chief et al., 2012). Post-fire reduction in $D_b$ is uncommon; however, a post-fire reduction in bulk density of 0.091 g cm$^{-3}$ was also observed in a Western Oregon Cascades site that was burned during the 2020 Holiday Farm Fire (McCool et al., 2023) and is consistent with our observations of a 0.10 g cm$^{-3}$ difference in $D_b$ between the unburned and high burn severity sites. Additionally, a greater presence of burned-out or decaying roots in the burned soils could have increased the presence of mesopore preferential flow paths that have been shown to increase $K_{fs}$ (Lei et al., 2022). Much of the ash was incorporated into the surface soils at the burned sites, which can increase infiltration capacities (Larsen et al., 2009; Woods & Balfour, 2010) and may also explain the difference in $K_{fs}$, $S$, and $\Psi_f$, as the $S$ and $K_{fs}$ of wildfire ash are generally higher than mineral soil (Balfour & Woods, 2013).

Our study was not the first to report higher $K_{fs}$ 1-year post-fire; $K_{fs}$ was two times greater in a high severity burn than unburned in loam to sandy loam soils in Sichuan Province China (Lei et al., 2022). Similarly, following wildfire in chaparral, mixed conifer, and oak vegetation with sandy loam soils in central Arizona, $K_{fs}$ increased from 19 mm hr$^{-1}$ in unburned sites to 36 mm hr$^{-1}$ in the burned sites (Raymond et al., 2020). However, other soil hydraulic properties followed an opposite pattern, with $S$ three-times greater and $\Psi_f$ 15 times greater in unburned soils relative to burned soils (Raymond et al., 2020). The contrasting soil hydraulic properties between our study and the study from Arizona may indicate a difference in inherent water repellency between study regions or may be explained by differences in 3-D infiltration, which may overestimate the contribution of lateral infiltration in field soils, compared to 1-D infiltration through soil cores using a tension infiltrometer. Our measurements of $\Psi_f$ in both burned and unburned soils were consistent with values previously reported from fire-affected soils in California (Ebel & Moody, 2020), and the geometric mean of the $S^2/K_{fs}$ ratio for burned soils lies squarely within the "burned domain," while the $S^2/K_{fs}$ ratio for unburned soils is well below previously reported values for unburned soils (Ebel & Moody, 2017).

Inherent surface soil water repellency, which is common in soils of the western US (Doerr et al., 2009), may have influenced the low values for $K_{fs}$, $S$, and $\psi_f$ in the unburned soils. Although we did not quantify water repellency in

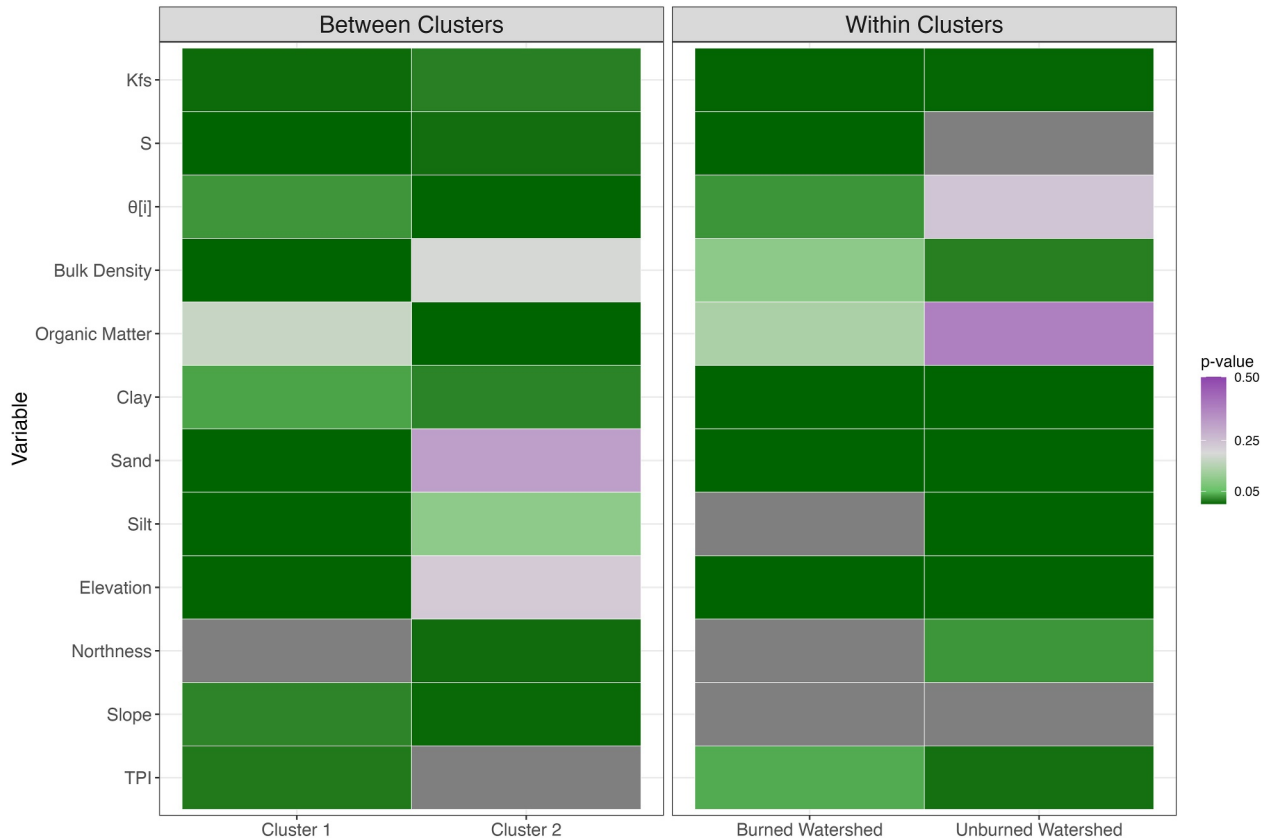


**Figure 8.** Kruskal-Wallis *p*-value heatmap for differences in burned and unburned samples between each cluster (left) and the difference between burned and unburned samples within each cluster (right). Green cells indicate *p*-values <0.05.

our soil samples, we qualitatively noted that unburned soil samples more frequently exhibited evidence of hydrophobicity compared to our burned soil samples. Previous research has demonstrated that wildfire can reduce or eliminate water repellency at the soil surface while potentially increasing subsurface repellency in areas with high background levels, such as in ash-capped soils in the Rocky Mountains (Robichaud et al., 2016). Inherent water repellency and feedback with initial soil water content may also explain a strong seasonal dependency on infiltration rates in unburned western Oregon Cascade forests (Johnson & Beschta, 1981), where summer infiltration rates have been observed to be 25%–50% lower than autumnal rates. Similar seasonal variations tied to soil moisture have been observed following wildfires in Northern California (Perkins et al., 2022) and Arizona (Martinez et al., 2025). Our soil samples were collected in the summer following an extended period with no wetting rains, which was reflected in the low moisture content values. Thus, our results likely represent the lower end of the range of hydraulic properties of these soils.

Regionally, there are few studies on post-fire soil hydraulic properties in the Western Cascades of Oregon, USA, to which we can directly compare our results. However, in a study in the Oregon High Cascades, $K_{fs}$ and S for burned soils were found to be 23.6 mm $hr^{-1}$ and 36.53 mm $hr^{-1/2}$, respectively (Wall et al., 2020). Although $K_{fs}$ in the High Cascades was similar to the value observed in our burned sites (19.39 mm $hr^{-1}$), $S$ was significantly greater than our burned soil measurements (6.07 mm $hr^{-1/2}$) and was greater than other post-fire soils (Wall et al., 2020). However, the soil (sandy loam) and forest type, composed of mountain hemlock (*Tsuga mertensiana*) and Pacific silver fir (*Abies alba*), were different from those in our study area. Another study in the northwest Oregon Cascades measured $K_{fs}$ of 72.8 and 61.5 mm $hr^{-1}$ in two high burn severity locations approximately 1.5 years after a fire (Hammer, 2022), which further demonstrates the potential for high post-fire $K_{fs}$ in the Western Cascades forests dominated by Douglas-fir.

The post-fire increase in soil hydraulic properties observed in our study area is relatively unique compared to changes documented in other ecosystems, where decreases in hydraulic properties are more common. Reductions

reported in the literature range from 20% (Ebel & Moody, 2017) to 90% or more in $K_{fs}$ (Moody et al., 2016), and around 90% for $S$ (Ebel & Moody, 2017), with typical $K_{fs}$ burned/unburned ratios of 0.37 in fire-prone southern California (Ebel & Moody, 2020) and 0.4 in the American Rocky Mountains (Ebel, 2019; Larson-Nash et al., 2018; Martin & Moody, 2001). Our findings highlight the importance of considering that, under conditions of relatively low bulk density and relatively high organic matter content, soils may respond counterintuitively to the effects of wildfire, leading to increases in soil-hydraulic properties, potentially by altering pore size distribution and connectivity. Our findings also highlight the complicated interplay between changes in soil physical properties, which in concert with feedback between soil water repellency and initial soil moisture (Wondzell & King, 2003), may determine how soil-hydraulic properties respond to wildfire (Noske et al., 2016, 2022).

### 4.2. Spatial Distribution of Soil Hydraulic Properties

There was no clear relationship between burn severity and soil hydraulic properties. Although $K_{fs}$, $S$, and $\psi_f$ were generally lower in the low severity burn sites compared with the moderate and high severity burned sites, we found no spatial relation between burn severity and soil hydraulic properties. While previous studies have identified higher $K_{fs}$ with increasing topographic slope (Baiamonte et al., 2017; Casanova et al., 2000; Cerdà, 1996), our principal component and $k$-means cluster analysis showed that topographic variables, such as slope, aspect (northness) and topographic position were not important in explaining variations in $K_{fs}$ and $S$ in either burned or unburned soils. In prior studies, the slope dependence was attributed to increased crust (i.e., structural seal) development from raindrop splash impact in low slope areas, which likely did not occur at our unburned sites due to near-complete canopy closure and ground cover that prevented soil sealing or at the burned sites because of higher infiltration rates.

Topographic aspect has also been found to exert an influence on soil hydraulic properties, with lower infiltration rates on equatorial-facing slopes attributed to aspect-driven variability in vegetation type and soil thickness (Casanova et al., 2000; Cerdà, 1996). While aspect can indeed be a driver of vegetation and soil differences in other regions, we found no dependence of infiltration on aspect in our study. Our field observations indicated that vegetation composition and structure were relatively homogeneous across slope aspects, likely because the dense mixed-conifer overstory and similar site conditions dampened the expression of aspect related gradients. This observation is consistent with post-fire studies in Colorado, which also showed limited aspect effects under comparable forest canopies (Kinner & Moody, 2010). The moderate relief and low aridity in our study areas may also reduce the influence of aspect on hydrology (Fan et al., 2019).

### 4.3. Study Limitations

Our study has several key limitations. One is the small measurement footprint of the Mini Disk infiltrometer. The results of infiltration measurements may be dependent on the measurement scale (Langhans et al., 2016) due to the heterogeneous nature of soils. Negative pressure head was an important consideration when choosing a measurement method for our study, as positive pressure heads can overwhelm water repellent factors by exceeding positive water entry values (Feng et al., 2001; Wang et al., 2008) and will access larger preferential flow paths (Langhans et al., 2016) rather than infiltration through the soil matrix. Our results are therefore not directly comparable to other studies that used different measurement methods, such as rainfall simulators, constant positive pressure head permeameters, or falling head permeameters. Because untilled forest soils are highly heterogeneous, our soils almost certainly violate the homogeneity assumption of the equations for soil hydraulic properties (Vandervaere et al., 2000b), making our measurements empirical estimates of the soil's effective hydraulic properties.

Another potential source of error was the contact between the Mini Disk's porous metal plate and the soil. Although we attempted to ensure that the soil surface was even and free from coarse material and applied contact sand to enhance hydraulic connection between the Mini Disk and the soil surface, it was not possible for us to determine the exact percentage of the plate that was in contact with the soil. Additionally, we could not control for preferential flow paths from gaps in the soil along the core wall except when it was obvious in the infiltration data, such as a sudden increase in infiltration rate. We also did not capture the effects that the overlying unburned ground cover would have on infiltration due to the thickness of the organic layer (Franzluebbers, 2002).

### 4.4. Implications

The soil hydraulic property measurements taken in our study indicate that hydrological hazards, such as infiltration-excess driven erosion, flash floods, and runoff-triggered debris flows, may be less likely to occur within the first year post-fire than in other, more historically studied fire-prone regions, such as southern California and the Rocky Mountain region (McGuire et al., 2024; Selander et al., 2025; Wondzell & King, 2003). Our work suggests that regional calibration of post-fire soil hydrologic models is needed because our findings contrast with results from Colorado Front Range, California chaparral, and Australian dry eucalyptus environments on which models are currently parameterized (e.g., Ebel & Moody, 2020). These environments all have notably different climates, vegetation, soils, and geology compared to our Douglas-fir dominated study sites. Hence, our study illustrates the importance of undertaking additional research on post-fire soil hydraulic properties across various contrasting regions to enable the development of region-specific parameterization of models.

Our findings also provide insight into additional factors that may be essential for understanding and regionalizing post-wildfire soil-hydraulic property changes. We noted the importance of changes in bulk density, organic matter content, particle size distribution, initial soil water content, and soil water repellency; wildfire effects on these variables may determine the direction and magnitude of changes in soil-hydraulic properties at a given site. Our work showed a divergent response from prevailing expectations of post-wildfire decreases in soil-hydraulic properties; we found post-wildfire increases in soil-hydraulic properties under conditions of low bulk density and high organic matter content. Our findings suggest that bulk density and soil organic matter content, in concert with feedbacks between soil water repellency and initial soil moisture, may delineate thresholds of increasing versus decreasing soil hydraulic properties in response to wildfire. Future efforts of post-wildfire studies incorporating bulk density, organic matter content, particle size distribution, initial soil water content, ground cover, and soil water repellency in concert with soil hydraulic property measurements could prove crucial to unraveling regional differences and advancing prediction of post-wildfire hazards of flash floods and debris flows.

## 5. Conclusions

Our study measured soil hydraulic properties after the 2022 Cedar Creek Fire in the Oregon Western Cascades by collecting samples the following summer across a small burned and unburned watershed. Samples in the burned area had significantly greater field-saturated hydraulic conductivity ($K_{fs}$), sorptivity ($S$), and wetting front potential ($\Psi_f$) relative to unburned soil, yet there were no significant trends between burn severity classes, which was unexpected given trends from prior research. Clay content and bulk density decreased with increased burn severity, whereas organic matter content was not significantly different among burned soils but was greater than unburned soils. Higher organic matter, lower bulk density, and lower clay content tended to result in soils with greater infiltration capacities. These textural and density shifts also suggest an increase in effective pore sizes in burned soils, consistent with our interpretation that enhanced pore connectivity contributed to higher post-fire infiltration capacities. However, we found no relationship between soil physical and hydraulic properties and topographic variables other than watershed elevation. Additionally, while we did not quantify soil water repellency, qualitative observations in the field and laboratory were indicative of greater water repellency in unburned soils relative to burned soils. Therefore, future research could link objective measures of hydrophobicity, such as the molarity of the ethanol droplet test, to soil hydraulic properties in both unburned and burned soils of the coastal Pacific Northwest region, as well as explore seasonal variations in infiltration due to the strong seasonal variability in precipitation. Moreover, the results from our study highlight the need for region-specific post-wildfire hydrologic frameworks, especially as wildfires more frequently affect low aridity watersheds. Our results also underscore the critical importance of future work across different regions to link wildfire effects on soil hydraulic properties, infiltration and runoff processes, and water quantity and quality responses at the watershed scale.

## Conflict of Interest

The authors declare no conflicts of interest relevant to this study.

## Availability Statement

All of the soil data collected in this study and necessary to reproduce the analysis and figures are archived at the Oregon State University Scholar's Archive via Pimont et al. (2025).

**Acknowledgments**

We thank Brenna Cody, Weylin Crouch, Bradley Gerdes, Cossette Miller, Josiah Nelson, Emily Nussdorfer, and Paige Scott for field and laboratory assistance. We also thank Corina Cerovski-Darriau, Natalie Latysh, and two anonymous reviewers for their thoughtful comments on this manuscript. This research was partially funded by NASA through the ROSES program (Grant 141063 SPC004532). Additionally, the research, analysis and other work documented in this publication was partially funded by the USDA Forest Service through Agreement 22-JV-11261952-071; however, the findings, conclusions, and views expressed are those of the author(s) and do not necessarily represent the views of the USDA Forest Service. Any use of trade, firm, or product names is for descriptive purposes only and does not imply endorsement by the U.S. Government.

## References

Abatzoglou, J. T., & Williams, A. P. (2016). Impact of anthropogenic climate change on wildfire across western US forests. *Proceedings of the National Academy of Sciences*, *113*(42), 11770–11775. https://doi.org/10.1073/pnas.1607171113

Adams, M. A. (2013). Mega-fires, tipping points and ecosystem services: Managing forests and woodlands in an uncertain future. *Forest Ecology and Management*, *294*, 250–261. https://doi.org/10.1016/j.foreco.2012.11.039

Agee, J. (1998). The landscape ecology of western forest fire regimes. *Northwest Science*, *72*(January), 24–34.

Baiamonte, G., Bagarello, V., D'Asaro, F., & Palmeri, V. (2017). Factors influencing point measurement of near-surface saturated soil hydraulic conductivity in a small Sicilian basin. *Land Degradation & Development*, *28*(3), 970–982. https://doi.org/10.1002/ldr.2674

Balfour, V. N., & Woods, S. W. (2013). The hydrological properties and the effects of hydration on vegetative ash from the northern rockies, USA. *Catena*, *111*(December), 9–24. https://doi.org/10.1016/j.catena.2013.06.014

Beyene, M. T., Leibowitz, S. G., & Pennino, M. J. (2021). Parsing weather variability and wildfire effects on the post-fire changes in daily stream flows: A quantile-based statistical approach and its application. *Water Resources Research*, *57*(10), e2020WR028029. https://doi.org/10.1029/2020wr028029

Bisson, P. A., Rieman, B. E., Luce, C., Hessburg, P. F., Lee, D. C., Kershner, J. L., et al. (2003). Fire and aquatic ecosystems of the western USA: Current knowledge and key questions. *Forest Ecology and Management*, *178*(1–2), 213–229. https://doi.org/10.1016/s0378-1127(03)00063-x

Bladon, K. D., Emelko, M. B., Silins, U., & Stone, M. (2014). *Wildfire and the future of water supply*. ACS Publications.

Borah, D. K. (2011). Hydrologic procedures of storm event watershed models: A comprehensive review and comparison. *Hydrological Processes*, *25*(22), 3472–3489. https://doi.org/10.1002/hyp.8075

Burgy, R. H., & Scott, V. H. (1952). Some effects of fire and ash on the infiltration capacity of soils. *EOS Transactions of the American Geophysical Union*, *33*(3), 405–416.

Burkle, L. A., Myers, J. A., & Belote, R. T. (2015). Wildfire disturbance and productivity as drivers of plant species diversity across spatial scales. *Ecosphere*, *6*(10), 1–14. https://doi.org/10.1890/es15-00438.1

Cannon, S. H., & DeGraff, J. (2009). The increasing wildfire and post-fire debris-flow threat in western USA, and implications for consequences of climate change. In *Landslides–disaster risk reduction* (pp. 177–190). Springer.

Cannon, S. H., Gartner, J. E., Wilson, R. C., Bowers, J. C., & Laber, J. L. (2008). Storm rainfall conditions for floods and debris flows from recently burned areas in southwestern Colorado and southern California. *Geomorphology*, *96*(3–4), 250–269. https://doi.org/10.1016/j.geomorph.2007.03.019

Cardenas, M. B., & Kanarek, M. R. (2014). Soil moisture variation and dynamics across a wildfire burn boundary in a loblolly pine (Pinus taeda) forest. *Journal of Hydrology*, *519*, 490–502. https://doi.org/10.1016/j.jhydrol.2014.07.016

Casanova, M., Messing, I., & Joel, A. (2000). Influence of aspect and slope gradient on hydraulic conductivity measured by tension infiltrometer. *Hydrological Processes*, *14*(1), 155–164. https://doi.org/10.1002/(sici)1099-1085(200001)14:1<155::aid-hyp917>3.0.co;2-j

Cerdà, A. (1996). Seasonal variability of infiltration rates under contrasting slope conditions in southeast Spain. *Geoderma*, *69*(3–4), 217–232. https://doi.org/10.1016/0016-7061(95)00062-3

Cerdà, A., & Robichaud, P. R. (2009). Fire effects on soil infiltration. In *Fire effects on soils and restoration strategies* (pp. 81–103). CRC Press.

Chen, J., Pangle, L. A., Gannon, J. P., & Stewart, R. D. (2020). Soil water repellency after wildfires in the blue ridge mountains, United States. *International Journal of Wildland Fire*, *29*(11), 1009–1020. https://doi.org/10.1071/wf20055

Chief, K., Young, M. H., & Shafer, D. S. (2012). Changes in soil structure and hydraulic properties in a wooded-shrubland ecosystem following a prescribed fire. *Soil Science Society of America Journal*, *76*(6), 1965–1977. https://doi.org/10.2136/sssaj2011.0072

Daly, C., Taylor, G., & Gibson, W. (1997). The PRISM approach to mapping precipitation and temperature. In *Proc., 10th AMS conf. on applied climatology* (Vol. 675).

Dennison, P. E., Brewer, S. C., Arnold, J. D., & Moritz, M. A. (2014). Large wildfire trends in the western United States, 1984–2011. *Geophysical Research Letters*, *41*(8), 2928–2933. https://doi.org/10.1002/2014gl059576

Doerr, S., Shakesby, R., Blake, W., Chafer, C., Humphreys, G., & Wallbrink, P. (2006). Effects of differing wildfire severities on soil wettability and implications for hydrological response. *Journal of Hydrology*, *319*(1–4), 295–311. https://doi.org/10.1016/j.jhydrol.2005.06.038

Doerr, S., Woods, S., Martin, D., & Casimiro, M. (2009). Natural background'soil water repellency in conifer forests of the north-western USA: Its prediction and relationship to wildfire occurrence. *Journal of Hydrology*, *371*(1–4), 12–21. https://doi.org/10.1016/j.jhydrol.2009.03.011

dos Santos, R. C. V., Vargas, M. M., Timm, L. C., Beskow, S., Siqueira, T. M., Mello, C. R., et al. (2021). Examining the implications of spatial variability of saturated soil hydraulic conductivity on direct surface runoff hydrographs. *Catena*, *207*, 105693. https://doi.org/10.1016/j.catena.2021.105693

Ebel, B. A. (2013). Wildfire and aspect effects on hydrologic states after the 2010 Fourmile Canyon Fire. *Vadose Zone Journal*, *12*(1), vzj2012–vzj2089. https://doi.org/10.2136/vzj2012.0089

Ebel, B. A. (2019). Measurement method has a larger impact than spatial scale for plot-scale field-saturated hydraulic conductivity (Kfs) after wildfire and prescribed fire in forests. *Earth Surface Processes and Landforms*, *44*(10), 1945–1956. https://doi.org/10.1002/esp.4621

Ebel, B. A., Koch, J. C., & Walvoord, M. A. (2019). Soil physical, hydraulic, and thermal properties in interior Alaska, USA: Implications for hydrologic response to thawing permafrost conditions. *Water Resources Research*, *55*(5), 4427–4447. https://doi.org/10.1029/2018WR023673

Ebel, B. A., & Moody, J. A. (2017). Synthesis of soil-hydraulic properties and infiltration timescales in wildfire-affected soils. *Hydrological Processes*, *31*(2), 324–340. https://doi.org/10.1002/hyp.10998

Ebel, B. A., & Moody, J. A. (2020). Parameter estimation for multiple post-wildfire hydrologic models. *Hydrological Processes*, *34*(21), 4049–4066. https://doi.org/10.1002/hyp.13865

Ebel, B. A., Moody, J. A., & Martin, D. A. (2012). Hydrologic conditions controlling runoff generation immediately after wildfire. *Water Resources Research*, *48*(3). https://doi.org/10.1029/2011WR011470

Ebel, B. A., Moody, J. A., & Martin, D. A. (2022). Post-fire temporal trends in soil-physical and-hydraulic properties and simulated runoff generation: Insights from different burn severities in the 2013 Black Forest Fire, CO, USA. *Science of the Total Environment*, *802*, 149847. https://doi.org/10.1016/j.scitotenv.2021.149847

Ebel, B. A., Rengers, F. K., & Tucker, G. E. (2016). Observed and simulated hydrologic response for a first-order catchment during extreme rainfall 3 years after wildfire disturbance. *Water Resources Research*, *52*(12), 9367–9389. https://doi.org/10.1002/2016wr019110

Eidenshink, J., Schwind, B., Brewer, K., Zhu, Z.-L., Quayle, B., & Howard, S. (2007). A project for monitoring trends in burn severity. *Fire Ecology*, *3*(1), 3–21. https://doi.org/10.4996/fireecology.0301003

Emelko, M. B., Silins, U., Bladon, K. D., & Stone, M. (2011). Implications of land disturbance on drinking water treatability in a changing climate: Demonstrating the need for "source water supply and protection" strategies. *Water Research*, *45*(2), 461–472. https://doi.org/10.1016/j.watres.2010.08.051

Fan, Y., Clark, M., Lawrence, D. M., Swenson, S., Band, L. E., Brantley, S. L., et al. (2019). Hillslope hydrology in global change research and earth system modeling. *Water Resources Research*, *55*(2), 1737–1772. https://doi.org/10.1029/2018WR023903

Feng, G., Letey, J., & Wu, L. (2001). Water ponding depths affect temporal infiltration rates in a water-repellent sand. *Soil Science Society of America Journal*, *65*(2), 315–320. https://doi.org/10.2136/sssaj2001.652315x

Feng, S., & Vardanega, P. J. (2019). A database of saturated hydraulic conductivity of fine-grained soils: Probability density functions. *Georisk: Assessment and Management of Risk for Engineered Systems and Geohazards*, *13*(4), 255–261. https://doi.org/10.1080/17499518.2019.1652919

Franzluebbers, A. J. (2002). Water infiltration and soil structure related to organic matter and its stratification with depth. *Soil and Tillage Research*, *66*(2), 197–205. https://doi.org/10.1016/s0167-1987(02)00027-2

Gerke, K. M., Khirevich, S., Vasilyev, R. V., Karsanina, M. V., Umarova, A. B., Barbosa, L. A. P., et al. (2026). Soil hydraulic properties derived from pore-scale simulations: Digital assessment of Ksat through model intercomparison and verification with experimental data. *Soil and Tillage Research*, *255*, 106790. https://doi.org/10.1016/j.still.2025.106790

Guo, Y., & Ma, C. (2023). Elucidating the role of soil hydraulic properties on aspect-dependent landslide initiation. *Hydrology and Earth System Sciences*, *27*(8), 1667–1682. https://doi.org/10.5194/hess-27-1667-2023

Hallema, D. W., Sun, G., Bladon, K. D., Norman, S. P., Caldwell, P. V., Liu, Y., & McNulty, S. G. (2017). Regional patterns of postwildfire streamflow response in the Western United States: The importance of scale-specific connectivity. *Hydrological Processes*, *31*(14), 2582–2598. https://doi.org/10.1002/hyp.11208

Hammer, M. N. (2022). *Post-fire erosional and hydrological processes promoting debris flow initiation in a Douglas fir and western hemlock forest in the riverside burn area, Oregon*. (Master's Thesis). Portland State University.

Heckman, K., Welty-Bernard, A., Rasmussen, C., & Schwartz, E. (2009). Geologic controls of soil carbon cycling and microbial dynamics in temperate conifer forests. *Chemical Geology*, *267*(1–2), 12–23. https://doi.org/10.1016/j.chemgeo.2009.01.004

Hennig, C. (2007). Cluster-wise assessment of cluster stability. *Computational Statistics & Data Analysis*, *52*(1), 258–271. https://doi.org/10.1016/j.csda.2006.11.025

Hoch, O. J., McGuire, L. A., Youberg, A. M., & Rengers, F. K. (2021). Hydrogeomorphic recovery and temporal changes in rainfall thresholds for debris flows following wildfire. *Journal of Geophysical Research: Earth Surface*, *126*(12), e2021JF006374. https://doi.org/10.1029/2021jf006374

Holden, S. R., Berhe, A. A., & Treseder, K. K. (2015). Decreases in soil moisture and organic matter quality suppress microbial decomposition following a boreal forest fire. *Soil Biology and Biochemistry*, *87*, 1–9. https://doi.org/10.1016/j.soilbio.2015.04.005

Hoogsteen, M. J., Lantinga, E. A., Bakker, E. J., Groot, J. C., & Tittonell, P. A. (2015). Estimating soil organic carbon through loss on ignition: Effects of ignition conditions and structural water loss. *European Journal of Soil Science*, *66*(2), 320–328. https://doi.org/10.1111/ejss.12224

Hrelja, I., Šestak, I., & Bogunović, I. (2020). Wildfire impacts on soil physical and chemical properties-a short review of recent studies. *Agriculturae Conspectus Scientificus*, *85*(4), 293–301.

Huffman, E. L., MacDonald, L. H., & Stednick, J. D. (2001). Strength and persistence of fire-induced soil hydrophobicity under ponderosa and lodgepole pine, Colorado Front Range. *Hydrological Processes*, *15*(15), 2877–2892. https://doi.org/10.1002/hyp.379

Johnson, M. G., & Beschta, R. L. (1981). *Seasonal variation of infiltration capacities of soils in western Oregon* (Vol. 373). US Department of Agriculture, Forest Service.

Kaufman, L., & Rousseeuw, P. J. (2009). *Finding groups in data: An introduction to cluster analysis*. John Wiley & Sons.

Key, C., & Benson, N. (2005). *Landscape assessment: Remote sensing of severity, the normalized burn ratio and ground measure of severity, the composite burn index*. FIREMON: Fire Effects Monitoring and Inventory System Ogden, USDA Forest Service, Rocky Mountain Res. Station.108

Khirevich, S., Yutkin, M., & Patzek, T. W. (2022). Correct estimation of permeability using experiment and simulation. *Physics of Fluids*, *34*(12), 123603. https://doi.org/10.1063/5.0123673

Kinner, D., & Moody, J. (2010). Spatial variability of steady-state infiltration into a two-layer soil system on burned hillslopes. *Journal of Hydrology*, *381*(3–4), 322–332. https://doi.org/10.1016/j.jhydrol.2009.12.004

Langhans, C., Lane, P. N. J., Nyman, P., Noske, P. J., Cawson, J. G., Oono, A., & Sheridan, G. J. (2016). Scale-dependency of effective hydraulic conductivity on fire-affected hillslopes. *Water Resources Research*, *52*(7), 5041–5055. https://doi.org/10.1002/2016WR018998

Larsen, I. J., MacDonald, L. H., Brown, E., Rough, D., Welsh, M. J., Pietraszek, J. H., et al. (2009). Causes of post-fire runoff and erosion: Water repellency, cover, or soil sealing? *Soil Science Society of America Journal*, *73*(4), 1393–1407. https://doi.org/10.2136/sssaj2007.0432

Larson-Nash, S. S., Robichaud, P. R., Pierson, F. B., Moffet, C. A., Williams, C. J., Spaeth, K. E., et al. (2018). Recovery of small-scale infiltration and erosion after wildfires. *Journal of Hydrology and Hydromechanics*, *66*(3), 261–270. https://doi.org/10.1515/johh-2017-0056

Lei, M., Cui, Y., Ni, J., Zhang, G., Li, Y., Wang, H., et al. (2022). Temporal evolution of the hydromechanical properties of soil-root systems in a forest fire in China. *Science of the Total Environment*, *809*, 151165. https://doi.org/10.1016/j.scitotenv.2021.151165

Leij, F. J., Romano, N., Palladino, M., Schaap, M. G., & Coppola, A. (2004). Topographical attributes to predict soil hydraulic properties along a hillslope transect. *Water Resources Research*, *40*(2). https://doi.org/10.1029/2002wr001641

Liu, H., Lei, T., Zhao, J., Yuan, C., Fan, Y., & Qu, L. (2011). Effects of rainfall intensity and antecedent soil water content on soil infiltrability under rainfall conditions using the run off-on-out method. *Journal of Hydrology*, *396*(1–2), 24–32. https://doi.org/10.1016/j.jhydrol.2010.10.028

Liu, T., McGuire, L. A., Youberg, A. M., Gorr, A. N., & Rengers, F. K. (2023). Guidance for parameterizing post-fire hydrologic models with in situ infiltration measurements. *Earth Surface Processes and Landforms*, *48*(12), 2368–2386. https://doi.org/10.1002/esp.5633

Ma, Q., Bales, R. C., Rungee, J., Conklin, M. H., Collins, B. M., & Goulden, M. L. (2020). Wildfire controls on evapotranspiration in California's Sierra Nevada. *Journal of Hydrology*, *590*, 125364. https://doi.org/10.1016/j.jhydrol.2020.125364

Madsen, M., Zvirzdin, D., Petersen, S., Hopkins, B., Roundy, B., & Chandler, D. (2011). Soil water repellency within a burned piñon–juniper woodland: Spatial distribution, severity, and ecohydrologic implications. *Soil Science Society of America Journal*, *75*(4), 1543–1553. https://doi.org/10.2136/sssaj2010.0320

Martin, D. A., & Moody, J. A. (2001). Comparison of soil infiltration rates in burned and unburned mountainous watersheds. *Hydrological Processes*, *15*(15), 2893–2903. https://doi.org/10.1002/hyp.380

Martinez, J. R., McGuire, L. A., & Youberg, A. M. (2025). Insights into temporal changes in debris flow susceptibility following fire in the Southwest USA from monitoring and repeat estimates of soil hydraulic and physical properties. *Earth Surface Processes and Landforms*, *50*(2), e70015. https://doi.org/10.1002/esp.70015

Mataix-Solera, J., Cerdà, A., Arcenegui, V., Jordán, A., & Zavala, L. (2011). Fire effects on soil aggregation: A review. *Earth-Science Reviews*, *109*(1–2), 44–60. https://doi.org/10.1016/j.earscirev.2011.08.002

McCool, K. D., Holub, S. M., Gao, S., Morrissette, B. A., Blunn, J. E., Gallo, A. C., & Hatten, J. A. (2023). Quantifying impacts of forest fire on soil carbon in a young, intensively managed tree farm in the western Oregon Cascades. *Soil Science Society of America Journal*, *87*(6), 1458–1473. https://doi.org/10.1002/saj2.20582

McGuire, L. A., Ebel, B. A., Rengers, F. K., Vieira, D. C., & Nyman, P. (2024). Fire effects on geomorphic processes. *Nature Reviews Earth & Environment*, *5*(7), 486–503. https://doi.org/10.1038/s43017-024-00557-7

McGuire, L. A., Rengers, F. K., Kean, J. W., Staley, D. M., & Mirus, B. B. (2018). Incorporating spatially heterogeneous infiltration capacity into hydrologic models with applications for simulating post-wildfire debris flow initiation. *Hydrological Processes*, *32*(9), 1173–1187. https://doi.org/10.1002/hyp.11458

Mikutta, R., Kleber, M., Kaiser, K., & Jahn, R. (2005). Organic matter removal from soils using hydrogen peroxide, sodium hypochlorite, and disodium peroxodisulfate. *Soil Science Society of America Journal*, *69*(1), 120–135.

Moody, J. A., Ebel, B. A., Nyman, P., Martin, D. A., Stoof, C., & properties, R. M. (2016). Relations between soil hydraulic properties and burn severity. *International Journal of Wildland Fire*, *25*(3), 279–293. https://doi.org/10.1071/wf14062

Moody, J. A., & Martin, D. A. (2009). Forest fire effects on geomorphic processes. In *Fire effects on soils and restoration strategies* (pp. 41–79). CRC Press.

Moody, J. A., Martin, R. G., & Ebel, B. A. (2019). Sources of inherent infiltration variability in postwildfire soils. *Hydrological Processes*, *33*(23), 3010–3029. https://doi.org/10.1002/hyp.13543

Nanzyo, M., Shoji, S., & Dahlgren, R. (1993). Physical characteristics of volcanic ash soils. In *Developments in soil science* (Vol. 21, pp. 189–207). Elsevier. https://doi.org/10.1016/s0166-2481(08)70268-x

Neary, D. G. (2011). Impacts of wildfire severity on hydraulic conductivity in forest, woodland, and grassland soils. *Hydraulic Conductivity—Issues, Determination, and Application*, *7*, 123–142.

Noske, P. J., Lane, P. N. J., Nyman, P., Van der Sant, R. E., & Sheridan, G. J. (2022). Predicting post-wildfire overland flow using remotely sensed indicators of forest productivity. *Hydrological Processes*, *36*(12), e14769. https://doi.org/10.1002/hyp.14769

Noske, P. J., Nyman, P., Lane, P. N., & Sheridan, G. J. (2016). Effects of aridity in controlling the magnitude of runoff and erosion after wildfire. *Water Resources Research*, *52*(6), 4338–4357. https://doi.org/10.1002/2015wr017611

Nyman, P., Sheridan, G., & Lane, P. N. J. (2010). Synergistic effects of water repellency and macropore flow on the hydraulic conductivity of a burned forest soil, south-east Australia. *Hydrological Processes*, *24*(20), 2871–2887. https://doi.org/10.1002/hyp.7701

Nyman, P., Sheridan, G. J., Smith, H. G., & Lane, P. N. (2011). Evidence of debris flow occurrence after wildfire in upland catchments of south-east Australia. *Geomorphology*, *125*(3), 383–401. https://doi.org/10.1016/j.geomorph.2010.10.016

Nyman, P., Sheridan, G. J., Smith, H. G., & Lane, P. N. (2014). Modeling the effects of surface storage, macropore flow and water repellency on infiltration after wildfire. *Journal of Hydrology*, *513*, 301–313. https://doi.org/10.1016/j.jhydrol.2014.02.044

Nyman, P., Yeates, P., Langhans, C., Noske, P. J., Peleg, N., Schärer, C., et al. (2021). Probability and consequence of postfire erosion for treatability of water in an unfiltered supply system. *Water Resources Research*, *57*(1), 2019WR026185. https://doi.org/10.1029/2019WR026185

Parks, S. A., Coop, J. D., & Davis, K. T. (2025). Intensifying fire season aridity portends ongoing expansion of severe wildfire in western US forests. *Global Change Biology*, *31*(8), e70429. https://doi.org/10.1111/gcb.70429

Peel, M. C., Finlayson, B. L., & Hydrology, T. A. M. (2007). Updated world map of the K\'f6ppen-Geiger climate classification. *Hydrology and Earth System Sciences*, *11*.

Perkins, J. P., Diaz, C., Corbett, S. C., Cerovski-Darriau, C., Stock, J. D., Prancevic, J. P., et al. (2022). Multi-stage soil-hydraulic recovery and limited ravel accumulations following the 2017 nuns and tubbs wildfires in northern California. *Journal of Geophysical Research: Earth Surface*, *127*(6), e2022JF006591. https://doi.org/10.1029/2022JF006591

Perry, D. A., Hessburg, P. F., Skinner, C. N., Spies, T. A., Stephens, S. L., Taylor, A. H., et al. (2011). The ecology of mixed severity fire regimes in Washington, Oregon, and Northern California. *Forest Ecology and Management*, *262*(5), 703–717. https://doi.org/10.1016/j.foreco.2011.05.004

Pimont, C., Bladon, K. D., & Thaler, E. A. (2025). Hydraulic properties of soils in burned and unburned watersheds in western Oregon following the 2022 cedar Creek fire. https://doi.org/10.7267/w3763h04c

Poon, P. K., & Kinoshita, A. M. (2018). Spatial and temporal evapotranspiration trends after wildfire in semi-arid landscapes. *Journal of Hydrology*, *559*, 71–83. https://doi.org/10.1016/j.jhydrol.2018.02.023

Raymond, C. A., McGuire, L. A., Youberg, A. M., Staley, D. M., & Kean, J. W. (2020). Thresholds for post-wildfire debris flows: Insights from the pinal fire, Arizona, USA. *Earth Surface Processes and Landforms*, *45*(6), 1349–1360. https://doi.org/10.1002/esp.4805

Rengers, F. K., McGuire, L. A., Kean, J. W., Staley, D. M., & flood, D. E. J. H. (2016). Model simulations of flood and debris flow timing in steep catchments after wildfire. *Water Resources Research*, *52*(8), 6041–6061. https://doi.org/10.1002/2015wr018176

Robichaud, P. R. (2000). Fire effects on infiltration rates after prescribed fire in Northern Rocky Mountain forests, USA. *Journal of Hydrology*, *231*, 220–229. https://doi.org/10.1016/s0022-1694(00)00196-7

Robichaud, P. R., Wagenbrenner, J. W., Pierson, F. B., Spaeth, K. E., Ashmun, L. E., & Moffet, C. A. (2016). Infiltration and interrill erosion rates after a wildfire in western Montana, USA. *Catena*, *142*, 77–88. https://doi.org/10.1016/j.catena.2016.01.027

Robinne, F.-N., Hallema, D. W., Bladon, K. D., Flannigan, M. D., Boisramé, G., Bréthaut, C. M., et al. (2021). Scientists' warning on extreme wildfire risks to water supply. *Hydrological Processes*, *35*(5), e14086. https://doi.org/10.1002/hyp.14086

Rust, A. J., Hogue, T. S., Saxe, S., & McCray, J. (2018). Post-fire water-quality response in the western United States. *International Journal of Wildland Fire*, *27*(3), 203–216. https://doi.org/10.1071/wf17115

Santín, C., Doerr, S. H., Preston, C. M., & González-Rodríguez, G. (2015). Pyrogenic organic matter production from wildfires: A missing sink in the global carbon cycle. *Global Change Biology*, *21*(4), 1621–1633. https://doi.org/10.1111/gcb.12800

Selander, B. D., Calhoun, N., Burns, W. J., Kean, J. W., & burned, F. K. R. (2025). Assessment of western Oregon debrisflow hazards in burned and unburned environments. *Earth Surface Processes and Landforms*, *50*(4), e70045. https://doi.org/10.1002/esp.70045

Shakesby, R. A., & Doerr, S. H. (2006). Wildfire as a hydrological and geomorphological agent. *Earth-Science Reviews*, *74*(3–4), 269–307. https://doi.org/10.1016/j.earscirev.2005.10.006

Sheridan, G. J., Lane, P. N., & Noske, P. J. (2007). Quantification of hillslope runoff and erosion processes before and after wildfire in a wet Eucalyptus forest. *Journal of Hydrology*, *343*(1–2), 12–28. https://doi.org/10.1016/j.jhydrol.2007.06.005

Sheridan, G. J., Nyman, P., Langhans, C., Cawson, J., Noske, P. J., Oono, A., et al. (2016). Is aridity a high-order control on the hydro–geomorphic response of burned landscapes? *International Journal of Wildland Fire*, *25*(3), 262–267. https://doi.org/10.1071/wf14079

Shillito, R. M., Berli, M., & Ghezzehei, T. A. (2020). Quantifying the effect of subcritical water repellency on sorptivity: A physically based model. *Water Resources Research*, *56*(11), e2020WR027942. https://doi.org/10.1029/2020wr027942

Smith, H. G., Sheridan, G. J., Lane, P. N., Nyman, P., & Haydon, S. (2011). Wildfire effects on water quality in forest catchments: A review with implications for water supply. *Journal of Hydrology*, *396*(1–2), 170–192. https://doi.org/10.1016/j.jhydrol.2010.10.043

Soil Survey Staff, Natural Resources Conservation Service. (2026). Web soil Survey. Retrieved from http://websoilsurvey.sc.egov.usda.gov/

Talsma, T., & Hallam, P. (1980). Hydraulic conductivity measurement of forest catchments. *Soil Research*, *18*(2), 139–148. https://doi.org/10.1071/sr9800139

Tibshirani, R., Walther, G., & Hastie, T. (2001). Estimating the number of clusters in a data set via the gap statistic. *Journal of the Royal Statistical Society: Series B*, *63*(2), 411–423. https://doi.org/10.1111/1467-9868.00293

Van der Sant, R. E., Nyman, P., Noske, P. J., Langhans, C., Lane, P. N., & Sheridan, G. J. (2018). Quantifying relations between surface runoff and aridity after wildfire. *Earth Surface Processes and Landforms*, *43*(10), 2033–2044. https://doi.org/10.1002/esp.4370

Vandervaere, J.-P., Vauclin, M., & Elrick, D. E. (2000a). Transient flow from tension infiltrometers I. The two-parameter equation. *Soil Science Society of America Journal*, *64*(4), 1263–1272. https://doi.org/10.2136/sssaj2000.6441263x

Vandervaere, J.-P., Vauclin, M., & Elrick, D. E. (2000b). Transient flow from tension infiltrometers II. Four methods to determine sorptivity and conductivity. *Soil Science Society of America Journal*, *64*(4), 1272–1284. https://doi.org/10.2136/sssaj2000.6441272x

Varela, M., Benito, E., & Keizer, J. (2015). Influence of wildfire severity on soil physical degradation in two pine forest stands of NW Spain. *Catena*, *133*, 342–348. https://doi.org/10.1016/j.catena.2015.06.004

Vieira, D., Fernández, C., Vega, J., & Keizer, J. (2015). Does soil burn severity affect the post-fire runoff and interrill erosion response? A review based on meta-analysis of field rainfall simulation data. *Journal of Hydrology*, *523*, 452–464. https://doi.org/10.1016/j.jhydrol.2015.01.071

Wall, S., Roering, J., & Rengers, F. K. (2020). Runoff-initiated post-fire debris flow Western Cascades, Oregon. *Landslides*, *17*(7), 1649–1661. https://doi.org/10.1007/s10346-020-01376-9

Wang, T., Zlotnik, V. A., Wedin, D., & Wally, K. D. (2008). Spatial trends in saturated hydraulic conductivity of vegetated dunes in the Nebraska Sand Hills: Effects of depth and topography. *Journal of Hydrology*, *349*(1–2), 88–97. https://doi.org/10.1016/j.jhydrol.2007.10.027

Weatherholt, J. A., & Johnson, B. G. (2024). Evaluating the occurrence and spatial patterns of soil water repellency in the Deschutes National Forest, Oregon. *Soil Science Society of America Journal*, *88*(4), 1014–1026. https://doi.org/10.1002/saj2.20666

Weiss, A. (2001). Topographic position and landforms analysis. In *Poster presentation, ESRI user conference* (Vol. 200).

Westerling, A. L. R. (2016). Increasing western US forest wildfire activity: Sensitivity to changes in the timing of spring. *Philosophical Transactions of the Royal Society B: Biological Sciences*, *371*(1696), 20150178. https://doi.org/10.1098/rstb.2015.0178

Westerling, A. L., Hidalgo, H. G., Cayan, D. R., & Swetnam, T. W. (2006). Warming and earlier spring increase western US forest wildfire activity. *Science*, *313*(5789), 940–943. https://doi.org/10.1126/science.1128834

White, I., & Sully, M. (1987). Macroscopic and microscopic capillary length and time scales from field infiltration. *Water Resources Research*, *23*(8), 1514–1522. https://doi.org/10.1029/wr023i008p01514

Wieting, C., Ebel, B. A., & Singha, K. (2017). Quantifying the effects of wildfire on changes in soil properties by surface burning of soils from the Boulder Creek Critical Zone Observatory. *Journal of Hydrology: Regional Studies*, *13*, 43–57. https://doi.org/10.1016/j.ejrh.2017.07.006

Williams, C. H., Silins, U., Spencer, S. A., Wagner, M. J., Stone, M., & Emelko, M. B. (2019). Net precipitation in burned and unburned subalpine forest stands after wildfire in the northern Rocky Mountains. *International Journal of Wildland Fire*, *28*(10), 750–760. https://doi.org/10.1071/wf18181

Wilson, G., Alfonsi, J. M., & Jardine, P. (1989). Spatial variability of saturated hydraulic conductivity of the subsoil of two forested watersheds. *Soil Science Society of America Journal*, *53*(3), 679–685. https://doi.org/10.2136/sssaj1989.03615995005300030005x

Wondzell, S. M., & King, J. G. (2003). Postfire erosional processes in the Pacific Northwest and Rocky Mountain regions. *Forest Ecology and Management*, *178*(1–2), 75–87. https://doi.org/10.1016/s0378-1127(03)00054-9

Woods, S. W., & Balfour, V. N. (2010). The effects of soil texture and ash thickness on the post-fire hydrological response from ash-covered soils. *Journal of Hydrology*, *393*(3–4), 274–286. https://doi.org/10.1016/j.jhydrol.2010.08.025

Woods, S. W., Birkas, A., & Ahl, R. (2007). Spatial variability of soil hydrophobicity after wildfires in Montana and Colorado. *Geomorphology*, *86*(3–4), 465–479. https://doi.org/10.1016/j.geomorph.2006.09.015